water

Article

Risk Assessment and Mapping of Flash Flood Vulnerable Zones in Arid Region, Fujairah City, UAE-Using Remote Sensing and GIS-Based Analysis

P. Subraelu [1,*], Alaa Ahmed [1,2], Abdel Azim Ebraheem [1], Mohsen Sherif [1,3], Shaher Bano Mirza [4], Fouad Lamghari Ridouane [4] and Ahmed Sefelnasr [1]

1 National Water and Energy Center, NWEC, United Arab Emirates University, Al Ain P.O. Box 15551, United Arab Emirates
2 Geosciences Department, United Arab Emirates University, Al Ain 15551, United Arab Emirates
3 Civil and Environmental Engineering Department, College of Engineering, United Arab Emirates University, Al Ain 15551, United Arab Emirates
4 Fujairah Research Center, Sakamkam Road, Fujairah P.O. Box 1626, United Arab Emirates
* Correspondence: subraelupakam@gmail.com

Abstract: A flash flood is the most common natural hazard that endangers people's lives, the economy, and infrastructure. Watershed management and planning are essential for reducing flood damages, particularly in residential areas, and mapping flash flood-sensitive zones. Flash flooding is an interface dynamic between geoterrain system factors such as geology, geomorphology, soil, drainage density, slope, and flood, rather than only water movement from higher to lower elevation. Consequently, the vulnerability to flash floods necessitates an awareness of and mapping topographical features. A flash flood vulnerable zones (FFVZ) map is essential for thorough flash flood risk assessment and management to minimize its detrimental effects, particularly in residential areas, especially in cities like Fujairah with seven wadis flowing into the city and even though it has two main dams and fifteen breaker dams. So, in this work, eight satellite image-derived parameters rainfall, elevation, slope, land use/land cover (LULC), drainage density, geology, geomorphology, and soil were combined to predict the flash flood-vulnerable zones using a weighted overlay technique based on geographic information systems (GIS). Each element of the thematic maps is ranked and weighted according to how vulnerable it is to flash floods in the study area, with 55 km^2 being classified as a very highly vulnerable area, 78 km^2 as a high-risk area, 9.3 km^2 as a moderate risk area, 70 km^2 as a low vulnerable area, and 257 km^2 as a very low vulnerable area. In addition, places with a very high vulnerability level include the Fujairah Airport, Fujairah Port, some residential neighborhoods in the city's center, oil storage areas, two hospitals, and universities. Additionally, from 1990 to the present, Landsat and Sentinel 2 data showed consistent changes in vegetation and built-up areas. Therefore, in addition to helping policy and decision-makers make the best choices about the efficacy of the study area's protective structures against the risk of flash floods in the future, the results can also be a valuable source of information.

Keywords: flash flood mapping; weighted overlay analysis; vulnerable zones; Geo-spatial analysis; GIS; remote sensing

check for updates

Citation: Subraelu P.; Ahmed, A.; Ebraheem, A.A.; Sherif, M.; Mirza, S.B.; Ridouane, F.L.; Sefelnasr, A. Risk Assessment and Mapping of Flash Flood Vulnerable Zones in Arid Region, Fujairah City, UAE-Using Remote Sensing and GIS-Based Analysis. *Water* **2023**, *15*, 2802. https://doi.org/10.3390/w15152802

Academic Editor: Chang Huang

Received: 6 July 2023
Revised: 23 July 2023
Accepted: 28 July 2023
Published: 2 August 2023

1. Introduction

The most frequent natural disasters globally are flash floods, which happen when a lot of rain falls quickly and produces a lot of surface runoff [1–3]. Flood catastrophes have frequently increased due to climate change and other environmental factors [4]. Since most nations are susceptible to flooding, it seriously threatens human life worldwide [5–10]. Flash floods can inflict damage anywhere, but they are especially destructive close to rivers and in agricultural areas, infrastructure, and human lives [11,12]. Globally, flash floods claim the lives of more than 5000 people each year [2,13]. Other factors, including drainage density and slope and a lack of efficient mapping or precautionary measures, may also contribute to this problem. Spatially explicit and catchment-scale flood models will be needed to evaluate landscape change and rainfall runoff scenarios to reduce the effects of flooding natural disasters and preserve healthy socio-ecological systems under changing catchment and climate conditions [14].

According to Jackson and Bates [15] and Sen [16], the Arabic word wadi refers to a dry valley stream generally found in desert regions, such as countries on the Arabian Peninsula. Earlier rainfall in Wadis is primarily episodic, fluctuating greatly in time and space, and many years go by without any rain. However, due to the effects of climate change, wadi flash floods in arid places have recently increased in frequency and severity [17,18]. According to [19], who examined pre- and post-flood scenarios using remotely sensed data, flash floods can produce enough runoff in direct response to intense and typically sudden rains for wadis to flow for some distance within the basin. However, the flow frequently does not reach the coast because of high transmission losses. According to the United Nations Office for Disaster Risk Reduction [20] (UNISDR), throughout the past 30 years, several disasters have affected Arabian countries, killed over 150,000 people and had an impact on almost 10 million others [21,22].

Flash floods, particularly in Oman, are frequently brought on by extreme events, such as tropical cyclones, that destroy enormous amounts of infrastructure and kill many people. In addition, Oman was affected by severe tropical cyclone Gonu in July 2007, which caused 54 fatalities and $3.9 billion in property damage [23,24]. Egypt has also had a series of flash floods in recent years, most notably in October 2019 and 2015. These floods caused devastating losses in terms of lives lost and property damage in Alexandria, Sinai, and Beheira [25,26]. The majority of the Middle East, including Jordan, Kuwait, Qatar, Saudi Arabia, United Arab Emirates (UAE), and Oman, saw severe destruction in October 2018 due to the increased frequency of intense rainfall events linked to numerous flash floods. These floods killed people and animals while destroying the primary infrastructures, including buildings, villages, agricultural lands, roads, electricity towers, and pipelines [27,28]. Wadi flooding in 2018 resulted in 4000 tourists fleeing to safer areas less than an hour before the peak flood hit Petra, Jordan's ancient landmark [29].

Additionally, it has been alleged that a flash flood in March 1966 caused roughly 200 fatalities and 250 injuries. Further, 3000 individuals are left homeless [30]. In the last ten years, severe flash floods have killed more than 113 people in Saudi Arabia and destroyed 10,000 dwellings [31]. Additionally, the northeastern section of the UAE, particularly Fujairah, has had a maximum of 13 floods during the past 20 years [32].

To further the discussion, nations in the Arabian Gulf region have invested in weather modification research and applications in response to the water resource problem, which is worsened by the region's expanding population and changing climate [33]. The UAE began running cloud seeding missions for additional rains to fulfil the country's expanding water needs in the previous decade, inspired by the global cloud seeding initiatives. The first of its sort began in the 1990s and modified how much precipitation clouds released [34]. The UAE government's official policy on cloud seeding began to be implemented significantly in 2010. This was unavoidable for an arid nation like the UAE, where average rainfall is less than 100 mm and high evaporation rates result in a lack of surface water and an overreliance on non-renewable groundwater resources that have caused aquifers to be depleted [35]. The Hajar Mountains in the eastern part of the UAE were specifically identified as having an apparent rise in rainfall intensities after comparing the pre-cloud seeding era (before 2010) and after [36]. Even though there is research available about the features of the UAE's rainfall, very few of these studies have looked into whether there is a connection between recent cloud-seeding missions and the rising rainfall intensities and urban flooding that have been seen.

The modeling of flash floods is a crucial tool for managing and mitigating floods [1,37–42]. Numerous studies have mapped flood-prone areas using a variety of methodologies, such as [9,43–46] have used traditional morphometric analyses. To prevent future property damage and fatalities from flash floods, flood control design must consider the effects of global warming, especially flash flood hazards in residential areas [47–49]. To initiate the flash flood vulnerable zones mapping, researchers used several hydrologic, geologic, biological, and climatic elements that affect flash floods in the catchment areas [3,13,39,50]. Geology, slope, LULC, drainage density, geomorphology, soil, distance to river, and rainfall distribution map are among the characteristics that are most crucial [51–53]. Aster satellite image data and GIS can be combined to create flood risk index maps, according to a study by [54]. Remote sensing is a useful method to track flood occurrences and pinpoint the hydrogeological settings without maps of flooded areas. The proliferation of satellites has also improved the likelihood of locating flooded areas. Flood risk maps were verified by [55] using free optical and radar satellite images. Eight characteristics, including rainfall, slope, drainage, soil, geological structures, geology, geomorphology, and land use and land cover, were utilized by [51] to simulate the flood danger. Getahun and Gebre [56] employed six variables to simulate the risk of flooding in the Awash River basin in Ethiopia. They used slope, elevation, rainfall, population density, land use, land cover, and soil type. Samanta [57] employed four parameters—elevation, slope, land use, and distance from the river—to create a model for flood danger maps in the vicinity of the Markham River in Papua New Guinea. Mathew Kelly [58] studied thoroughly to assess flood risk for Australia's Hawkesbury-Nepean Catchment. The number of characteristics needed to produce flood-vulnerable maps is generally not set; instead, it varies on the availability of data, the location of the study region, and the significance of the element.

Even though they can be deadly, flash floods can also be helpful because they replenish Fujairah City's parched aquifers and moisten the areas damaged by the drought, as UAE has limited conventional renewable water resources [59]. This type of natural hazard cannot be prevented, but it can be successfully controlled with the help of effective flood management strategies like harvesting floodwater and rainfall runoff for human and livestock use as well as agricultural growth while building subterranean dams, artificial lakes, recharge dams, and off-stream structures [25,60]. The main goal of this study was to identify the likely flash flood risk zones by examining all potential resource maps. By observing satellite images from the relevant period, the current work pinpoints areas prone to flash floods. GIS facilitates the administration and integration of multi-thematic data. Rainfall, elevation, slope, geology, geomorphology, LULC, soil, and drainage density are some of the thematic layers generated and examined via weighted overlay analysis for this study to identify potential flood-vulnerable areas. Flood-vulnerable maps provide local municipalities and citizens with information on the degree of flood danger in their communities. They can be utilized effectively as an evacuation guide during a flood event.

2. Study Area

With a total size of 1450 km^2, Fujairah is the fifth-largest emirate in the UAE [61]. The Emirate of Fujairah, one of the seven Sheikhdoms of the UAE, is the only emirate with its entire coastline situated on the Gulf of Oman and defined by a headland bay configuration with several cliffs extending into the Gulf [62]. Fujairah City is the capital of this emirate. The Hajar/Oman Mountains, which separate Fujairah from the Gulf of Oman and the Eastern Coastal Plain, are an exceptional feature of the emirate. The research area's highest point is 1103 m above mean sea level. This mountain is the source of numerous Wadis, including Wadi Hayl, wadi Saham, wadi Farfar, wadi Ham, wadi Yabsah, and Wadi Madhab, which flows into Fujairah City. The largest and longest wadi in the UAE, Wadi Ham, has a catchment area of 192 km^2 and extends over 30 km from Masafi in the northwest to the Wadi Ham Dam close to Fujairah City in the southeast. Wadi Saham, Wadi Farfar, and Wadi Yabsah finally debouches in Wadi Ham Dam (Figure 1). Most of the year, the wadi beds are dry, but when it rains, the dry wadi beds turn into rushing rivers, creating a breathtaking spectacle.

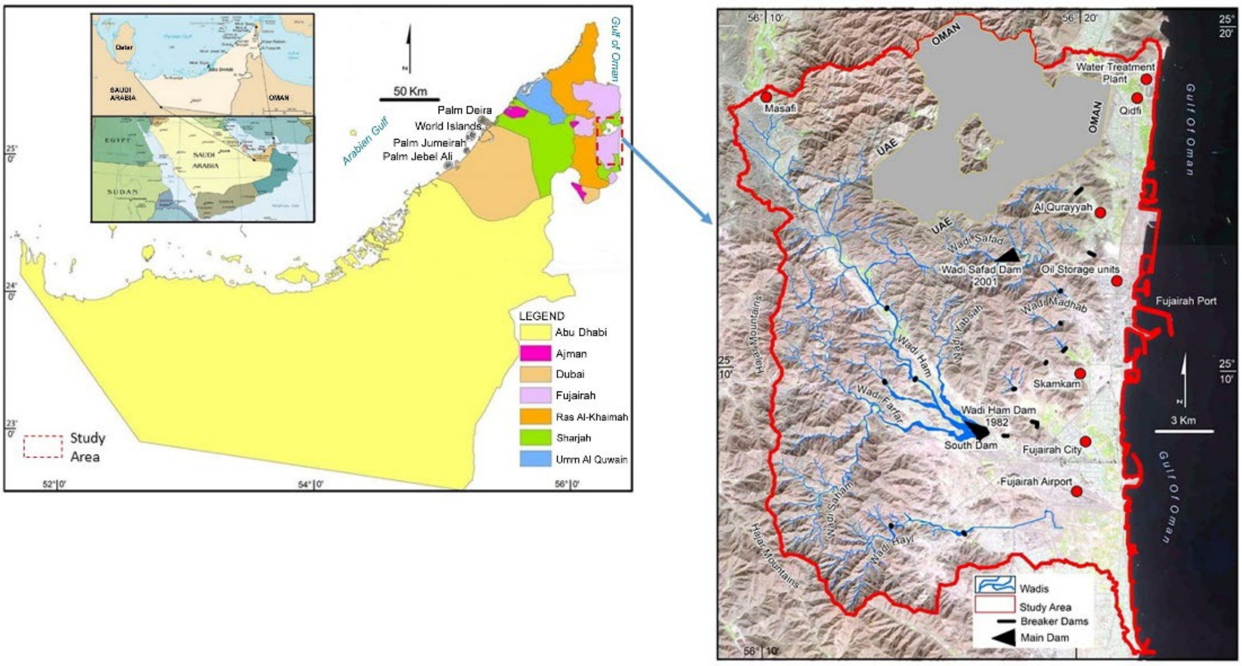

Figure 1. Location map of the study area showing the important areas in Fujairah City.

According to the demographic figures from the Fujairah Statistics Center (FSC) for 2023, 318,325 people are living in Fujairah, with Fujairah City (study area) housing over 77% of the total population [32]. Most of Fujairah City's urban areas are on low coastal plains, making them more vulnerable to flash floods. The UAE Ministry of Energy and Industry, in collaboration with the Ministry of Climate Change and Environment, has issued rules for protection against floods to lessen the effects of flash floods. When planning or building any residential area close to Wadis, they specified several requirements that had to be followed. These communities and government bodies will benefit from this paper's identification of flash flood vulnerable zones.

Fujairah is regarded as one of the UAE's most productive regions, along with the Hajar Mountains, the plains, and some desert regions. Major wadis drop through the Hajar Mountains on either side into the Fujairah, supplying significant floodwater to the neighboring alluvial and coastal plains. Fujairah City, which covers an area of around 559.86 km^2 between 25°17′ 31.63 N and 25°01′ 49.39 N and 56°08′ 50.73 N and 56°22′ 29.12 N, is included in the current research area, which is a section of the Fujairah emirate that consists of the catchment areas of the seven wadis. It mostly consists of the Fujairah City region, a portion of the Sharjah Emirate's Kalba and Khor Fakkan areas, and a 77 km^2 area of the Sultanate of Oman, as depicted in (Figure 1). In the northern and southern portions of the study area, the Fujairah city area is characterized by narrow coastal plains that range in width from 1 to 3 km and are at their widest in Al-Qurayyah and Skamkam. Lithologically, the Jurassic to Cretaceous igneous and metamorphic rocks are found in the north and west, and alluvial deposits at the foot of the mountains dominate the higher streams [63]. The study area experiences various meteorological conditions, including cold to mild in the winter and hot to humid in the summer. In the western mountainous regions, the annual rainfall ranges from 80 mm to 160 mm [64]. Approximately 97% of the total yearly rainfall in the northern section of the UAE was thought to fall over the eastern mountainous and coastal regions [64]. The region typically has dry weather with 100–250 mm precipitation per year [32,65–67]. During the winter and summer, Fujairah's typical temperatures range from 15 to 47 degrees Celsius.

3. Factors Leading to Study and Mapping the Flash Flood Vulnerable Zones in Fujairah City

The UAE has attracted many immigrants since its founding in 1973, who have significantly changed the country's geography. The demand for these individuals matched the economic growth from the massive oil profits [68]. Before 1980, Fujairah had an insignificant demographic situation, with a population of only 32,000. At this time, the majority of Fujairah city was made up of people who were mostly engaged in commerce and fishing. Since the current economic boom began 43 years ago, Fujairah Emirate's population has multiplied dramatically (Figure 2). Fujairah had 32,000 residents in 1980; that number has increased to 150,000 in 2010 and, by 2023, around 318,325. Based on its annual growth rate, Fujairah's population is among the fastest-growing in the region.

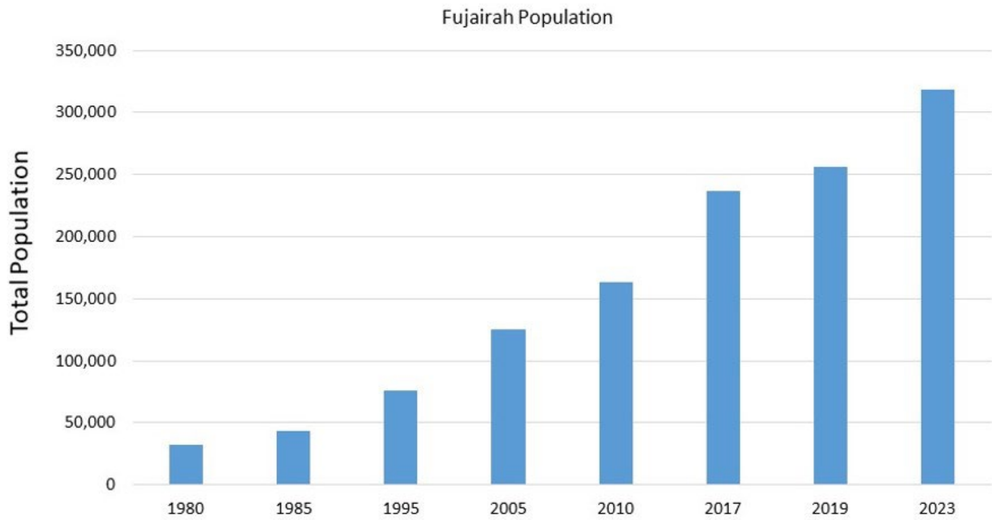

Figure 2. Bar graph showing the population of Fujairah from 1980–2023.

Regarding the study area, I, e, Fujairah City, which is 560 km^2, the Hajar Mountains occupy roughly 403 km^2 to the west. Therefore, the city of Fujairah's constantly growing population will have to reside in just 157 km^{2,} which is considered a challenge. As was already said, due to its closeness to the airport, schools, universities, shopping malls, and other significant facilities, over 77% of the population of the Fujairah emirate resides in Fujairah city [32].

Urban sprawl's extensive and rapid growth is a crucial indicator of population growth [69]. Increasing urban built-up areas and an increasing global population, particularly in coastal regions, have given rise to large cities. The LULC maps created with Landsat images from 1990, 2000, 2010, and Sentinel-2 from 2023 showed high levels of built-up growth in Fujairah (Figure 3). Urban waterlogging regions are growing more quickly and in size due to the expansion of urban sprawl, which has increased the impermeable surface area that prevents rain from penetrating the underlying soil. Over the previous 30 years, there has been a significant shift in the land use and cover in the Fujairah area (Figure 3), which could have increased the runoff coefficient. In the past 23 years, Fujairah City has seen more floods than any other place in the emirate of Fujairah, according to [32]. Other flooding causes include the extension of residential areas, making it harder for natural flows and drainage systems to remove surplus water after heavy rains. However, in recent years, human interference has given it a new dimension [70,71].

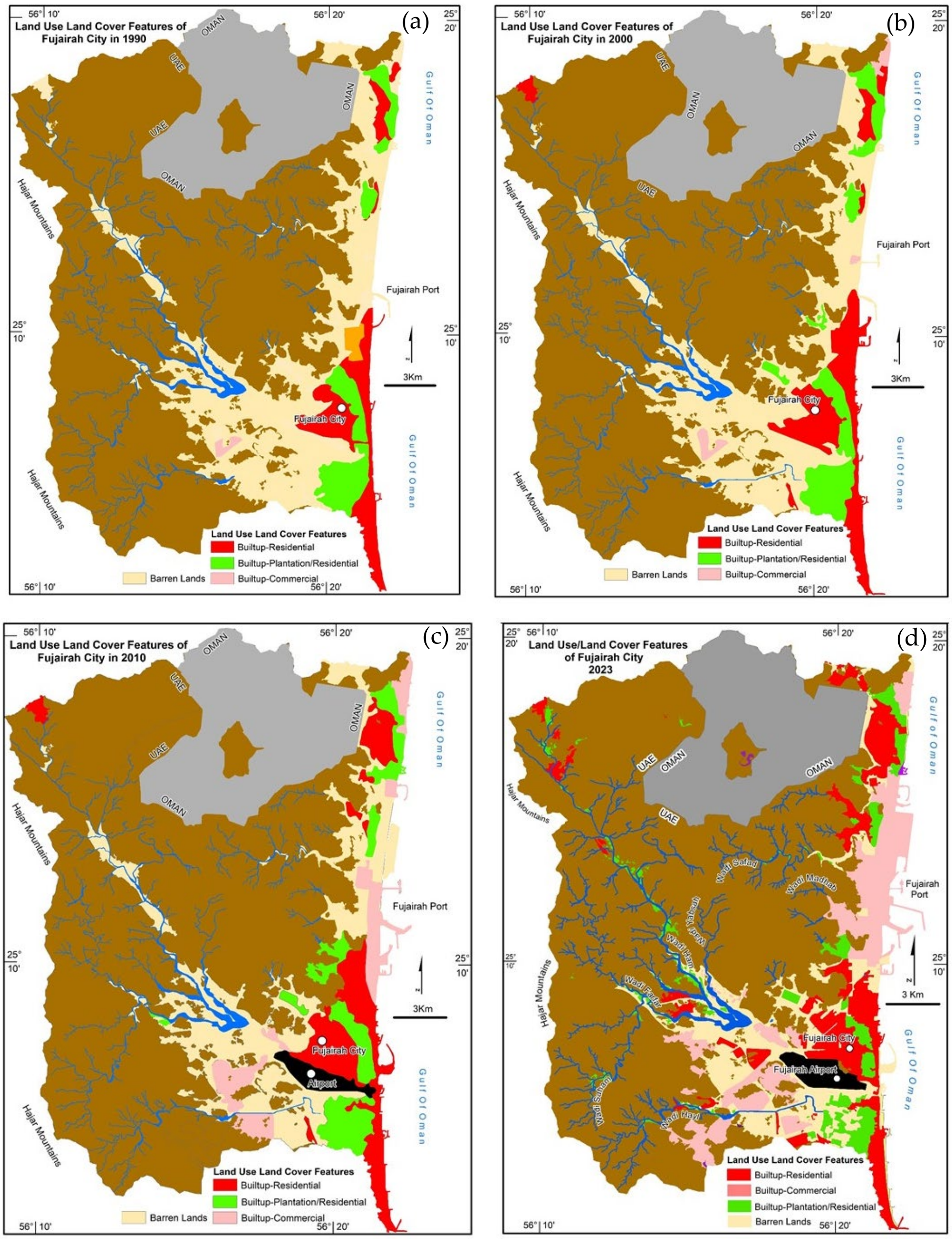

Figure 3. Maps showing the urban areas and vegetation in Fujairah City in (**a**) 1990, (**b**) 2000, (**c**) 2010, and (**d**) 2023.

As seen in Figure 3, the study area's built-up in 1990 covered an area of about 40 km^2, mostly in the south and northeastern parts of Fujairah City, mainly consisting of built-up residential and plantation areas. Urban sprawl reached 51 km^2 in 2000, with growth moving further to the north-western corner of the study area consisting of residential and plantation areas. The major change in the infrastructures (built-up) in the study area recorded from 2000 to 2023 is shown in Figure 4. The Fujairah Airport opened in 2010 due to tremendous development in Fujairah. During this time, the area of the Fujairah port expanded, as well as other significant commercial sectors, bringing the total built-up area to 88 km^2. Finally, the urban sprawl reached 115 km^2 in 2023, with most construction focused on growing residential areas to serve the continuously growing population, along with other facilities like shopping centers, universities, schools, etc.

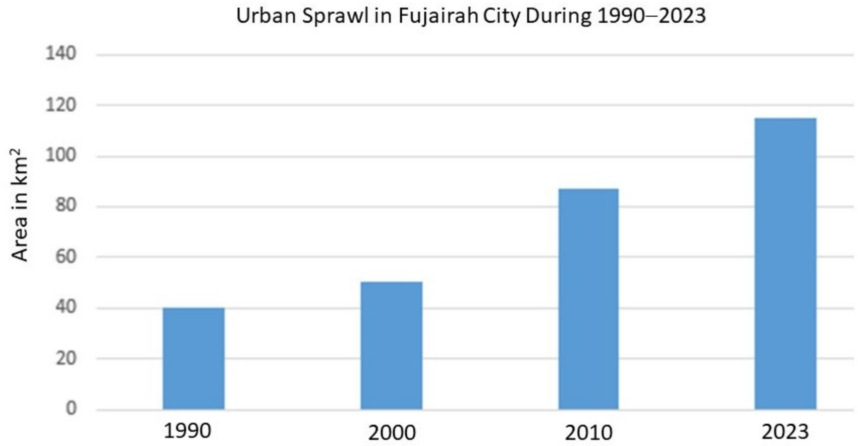

Figure 4. Urbanization trends in the study area.

The Northern part of UAE, which includes the study area, has recently seen multiple flash flooding incidents. Lately, the Eastern parts of UAE, Ras Al Khaimah (200 mm), Masafi (209.7 mm), and particularly Fujairah Port (inside the study area) recorded the highest rainfall of 234.9 mm, and Fujairah Airport with (153 mm), between the 25 July and 28 July 2022, according to reports on [72] The Gulf Today and The National News [73], respectively. Because of the unusually heavy rains and the presence of seven wadis in Fujairah City, namely Wadi Hayl, wadi Saham, wadi Farfar, wadi Ham, wadi Yabsah, wadi Madhab, and Wadi Safad (Figure 1), affecting total of 4225 people and were evacuated with the help of 1638 personnel who got affected by the flooding that occurred within these wadis and also water that was spilling over the southern side of the Wadi Ham Dam, which is inside the Fujairah city (Figure 5). Approximately 870 individuals were saved, and another 3897 people were given shelter [72] (Gulf Today, 2022). The world's third-largest fuel bunker canter, Fujairah Port, was also affected by widespread flooding [74].

Figure 5. Water flowed over the Wadi Ham South Dam during the floods of July 2022.

Similarly, to this, the floods had a significant negative impact on residential areas, agriculture/plantations, numerous automobiles, hospitals, schools, and electrical lines [75]. Since the majority of Fujairah City's key districts were affected, it is crucial to investigate the specific causes of these significant losses in addition to the high rainfall. This work has been done to identify flashflood-sensitive zones in Fujairah City while considering the seriousness of the problem.

4. Materials and Methods

The delineation of LULC features from the remote sensing satellite image Sentinel-2, 2023, which offers a revisit time of 10 days and a spatial resolution of 20 m and is retrieved from the Earth Resource Observation System, was the first of the eight thematic layers needed for this study. The ArcGIS Spatial Analyst module created other resource maps, such as drainage density, elevation, and slope, using SRTM DEM data. The additional thematic maps, such as a comprehensive geomorphology layer, geology, and soil layers, were created using Sentinel-2 images and referred to other works. The CHRS RainSphere website was utilized to gather rainfall data for the research area during the previous 22 years, which was then used to create a GIS layer for our analysis.

The overall methodology used for this study involves both spatial and non-spatial data collection. The spatial data are recorded in the database as several layers in digital form and include maps of drainage density, elevation, slope, geology, geomorphology, LULC, soil, and rainfall. All these layer integrations, queries, analyses, etc., are carried out in a GIS context. As a result, the new maps are accurately created by simply merging these layers and altering them to assess correlations between the selected features in the various layers under consideration.

This research utilized satellite images from the Earth Resource Observation system, specifically Landsat and Sentinel-2 images (Table 1). Landsat images from 1990, 2000, 2010, and Sentinel 2 for 2023 shed light on how the urban sprawl changed in Fujairah City over the years. Bands used in Landsat 7 and Landsat 5 are Band 4 Near-Infrared (0.77–0.90µm), Band 3 Red (0.63–0.69 µm), and Band 2 Green (0.52–0.60 µm) are used. For Sentinel-2, the bands used are Band 2 (Blue: 490 nm), Band 3 (Green: 560 nm) and Band 4 (665 nm). The land use/Land cover features in the study area have been interpreted and traced through onscreen digitization using level III standards of widely used National Remote Sensing Center (NRSC) classification are extracted to the extent discernible from these relatively high-resolution satellite images. All the Sentinel-2 images for the year 2023 were precisely geo-referenced, enhanced and smoothly mosaicked into a single image covering the Fujairah City area. The image mosaic is then subsequently subset with the study area layer.

Table 1. Data utilized for various parameters.

S. No	Map Layer	Data Used—Source
1	Rainfall	CHRS RainSphere (http://chrs.web.uci.edu) (accessed on 18 May 2023)
2	DEM	USGS-Earth Explorer website, 30 m resolution, (https://earthexplorer.usgs.gov/) (accessed on 25 April 2023)
3	Drainage Density	Derived from DEM
4	Elevation	Derived from DEM
5	Slope	Derived from DEM
6	Land use / Land cover	Sentinel-2 Satellite Image (2023), 20 m spatial resolution; dated 8 March 2023 Landsat 5 TM (1990) 30 m, spatial resolution; dated 19 Dec 1990 Landsat 5 TM (2000) 30 m, spatial resolution; dated 28 May 2000 Landsat 7 ETM (2010) 30 m, spatial resolution; dated 20 Sep 2010
7	Geology	Sentinel-2 satellite Image 20 m spatial resolution
8	Geomorphology	Sentinel-2 satellite Image 20 m spatial resolution
9	Soil	UAE—Soil Museum, https://www.emiratessoilmuseum.org (accessed on 18 May 2023)

The weighted overlay analysis combines data from several data categories. It applies analytical, statistical measurement, and other processes to the GIS data sets to turn the data into information applicable to a particular application. Using appropriate choice criteria and gradually layering one parameter over another, it is possible to integrate different themed maps. This operation entails computing regions, conducting logical operations, and superimposing several thematic maps. Themes from several satellite images, SRTM data, and supplementary data sets were translated into a raster format. Using ground control points, these raster images were painstakingly geo-rectified before being digitized on-screen with ArcGIS 10.4. To get better results from overlay analysis, these vectorized themes were placed in a GIS environment with uniform projection coordinates. Flood vulnerability maps were created based on each parameter's ranking and weights applied in overlay analysis [76]. Table 1 lists each layer's phenomenon, requirement, and source information. Final classifications include high, high, medium, low, and very low-risk areas for flash floods.

4.1. Parameters Responsible for Flash Floods

The result covers the creation of several resource input maps and the assessment of potential flood-vulnerable areas. To comprehend the flood dynamics of the research area, it is necessary to evaluate rainfall, DEM, and its derivatives, including elevation, slope, drainage density, LULC, geology, geomorphology, and soil.

4.1.1. Rainfall

The relationship between rainfall and flood occurrences in a region has been established by a significant body of prior literature [36,77–81]. The exact degree to which an increase in rainfall will result in flooding cannot be predicted [82]. Instead, it is possible to assert that rainfall is the primary cause of floods in all environmental contexts [83]. Numerous studies worldwide have chosen rainfall as one of the key influencing factors for mapping the risk of flash floods [14,84–86]. Rainfall in the study area ranges from 80 to 325 mm, with an average of 160 mm [87]. It is important to note that the rainiest months in this region are Oct–Apr (Figure 6) (CHRS, Rainsphere). CHRS Rainsphere is an integrated system for global satellite precipitation data and information developed by the center for Hydrometeorology and Remote Sensing at the University of Colorado, Irvine. From 2000 through 2022, the Fujairah City area's annual and monthly data is accessed from the website. When the annual data was closely examined (Figure 7), it was found that in the total 22 years, 14 of the years had an average rainfall of more than 100 mm and above, which is consistent with the flooding data given by [32] until 2018 and later also observed in 2019, 2020, and 2022. To create the rainfall isohyet map with the aid of ArcGIS software, the above rainfall data from the years 2000 to 2022 was used (Figure 8). The study area's 298 km^2 receives between 80 and 140 mm of rainfall, according to the rainfall isohyet map. 196 km^2 of the study area will receive rainfall between 140 and 160 mm, with the remaining 65 km^2 to the west of Fujairah City receiving more than 160 mm.

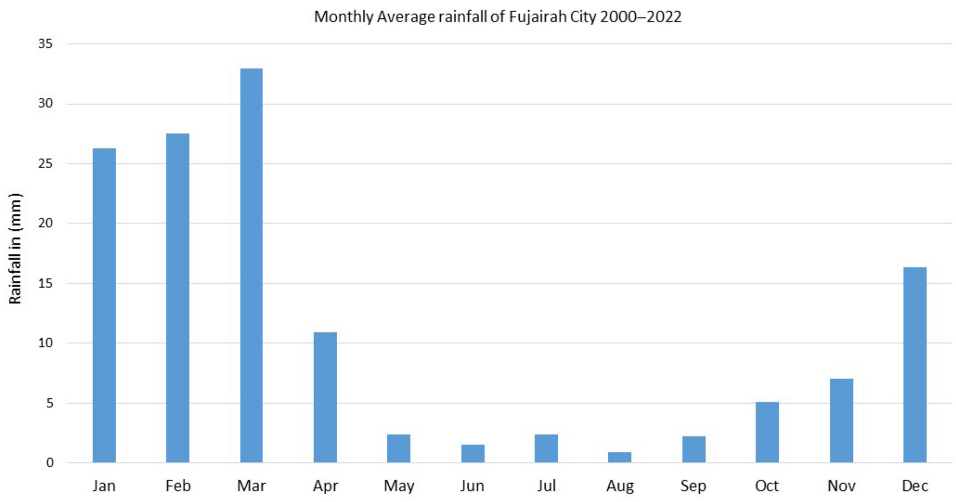

Figure 6. Monthly average rainfall of Fujairah City from 2000–2022.

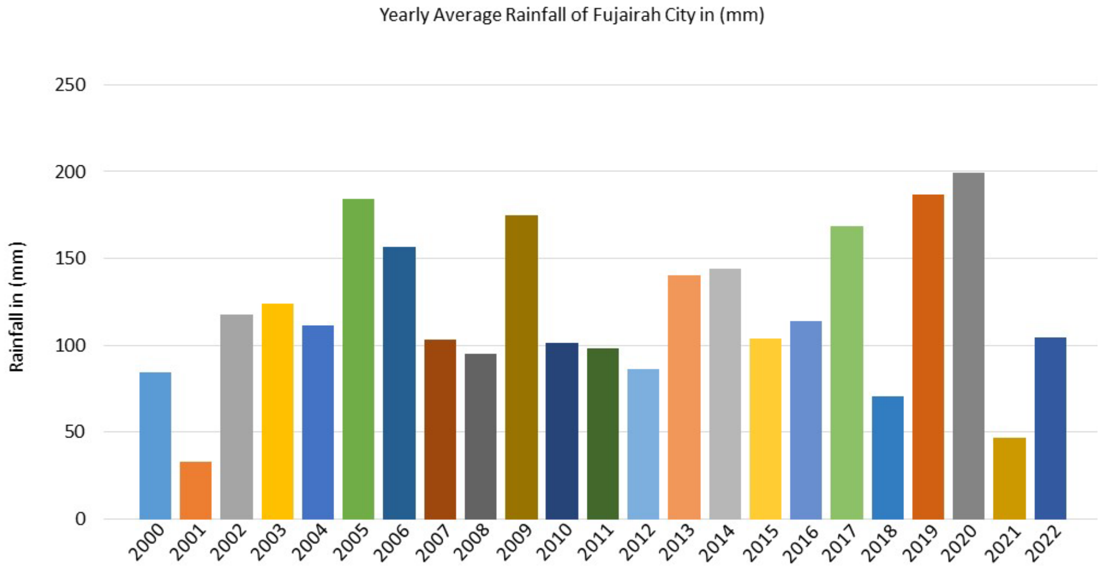

Figure 7. Yearly average rainfall of Fujairah City from (2000–2022).

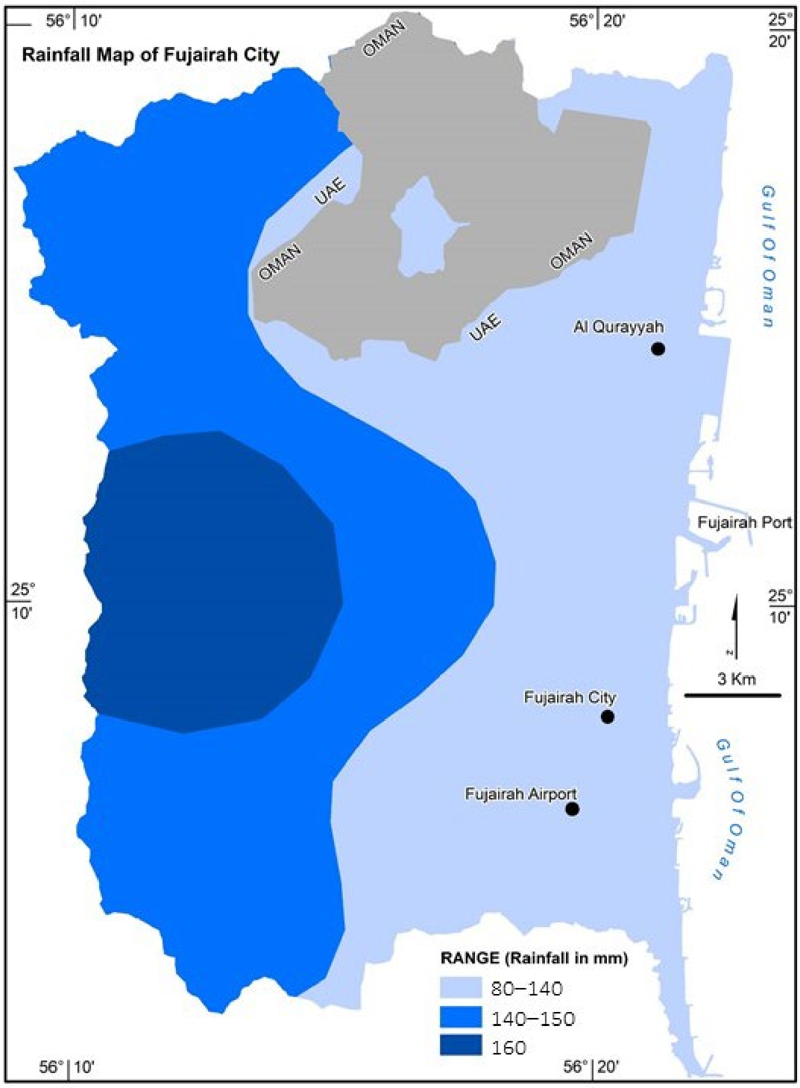

Figure 8. Average Rainfall map of Fujairah City.

4.1.2. Elevation

The classification is carried out using natural breaking in ArcGIS, and the elevation map is created using SRTM DEM of 30 m spatial resolution. The DEM and its derivatives are crucial in determining which regions are at risk of flooding. The research area's elevation and profile graph were produced from SRTM data and are displayed in Figure 9. Experts say elevation is the main factor in a region's ability to regulate floods [88–90]. Flat lowland places may flood more quickly than higher altitudes because water continuously flows from higher elevations to lower ones [91,92]. Most of the study area's built-up regions are lower than 50 m in elevation, rendering them more susceptible to flash flooding. In the study region, the elevation varies from 0 to 1100 m. Given that increased elevation decreases flash flooding risk, the entire range of elevation is divided into five rank classes ranging from 1 to 5. The ranks are assigned to various sections of the research region based on elevation for additional GIS analysis.

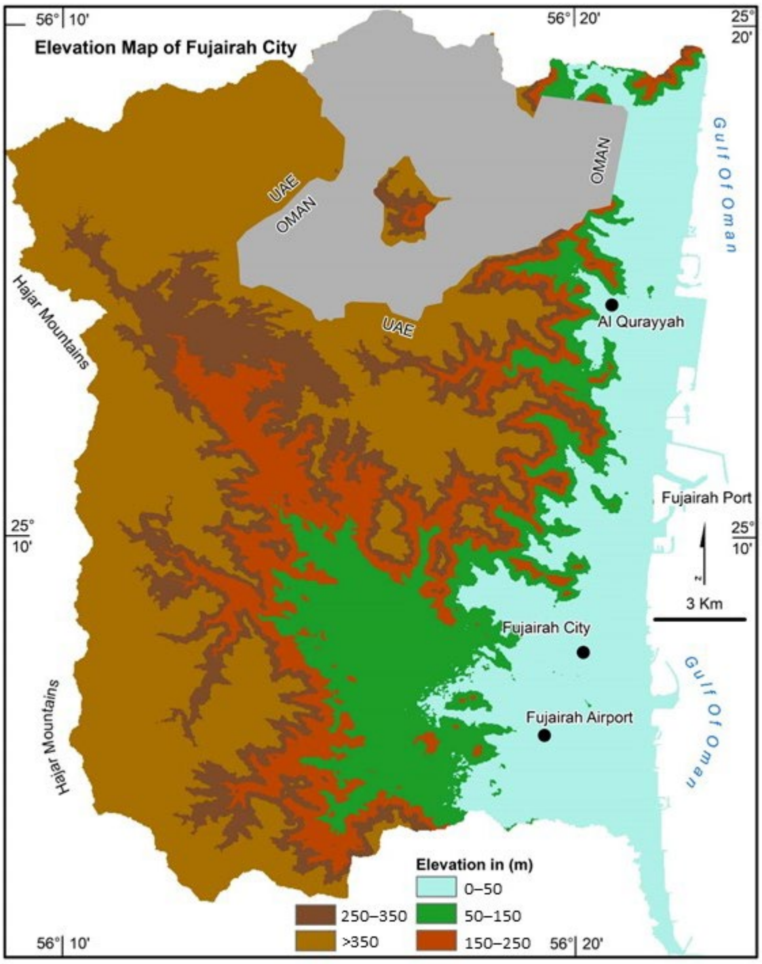

Figure 9. The elevation map of Fujairah City.

4.1.3. Slope

The slope of the research area indicates a crucial role in controlling surface discharge in hydrological assessment studies. The significance of this topographic feature has been noted by several researchers [84,88,90,93]. The slope of an area and the surface flow velocity have a significant positive link [91,94]. In addition, gradient influences infiltration to some extent. As the gradient rises, the surface runoff rises noticeably as well, which causes the infiltration to fall [91]. Due to the large amount of water that becomes immobile and generates a severe flood situation, places with a sudden fall in slope have a higher likelihood of flooding [88,95,96]. According to [97], a greater slope's size may hasten precipitation-related runoff. With the help of the 3D Analyst module in ArcGIS, the slope map is instantly generated from the SRTM DEM—the values of the slope range from 5% to 20%. The entire slope is divided into five classes, with the understanding that the lower the slope, which is less than 5%, the higher the vulnerability of the area, as shown in Figure 10, the higher the slope, more than <20% values lower the vulnerability wrt to flooding. Based on this, the ranks are assigned to all the areas in the study region.

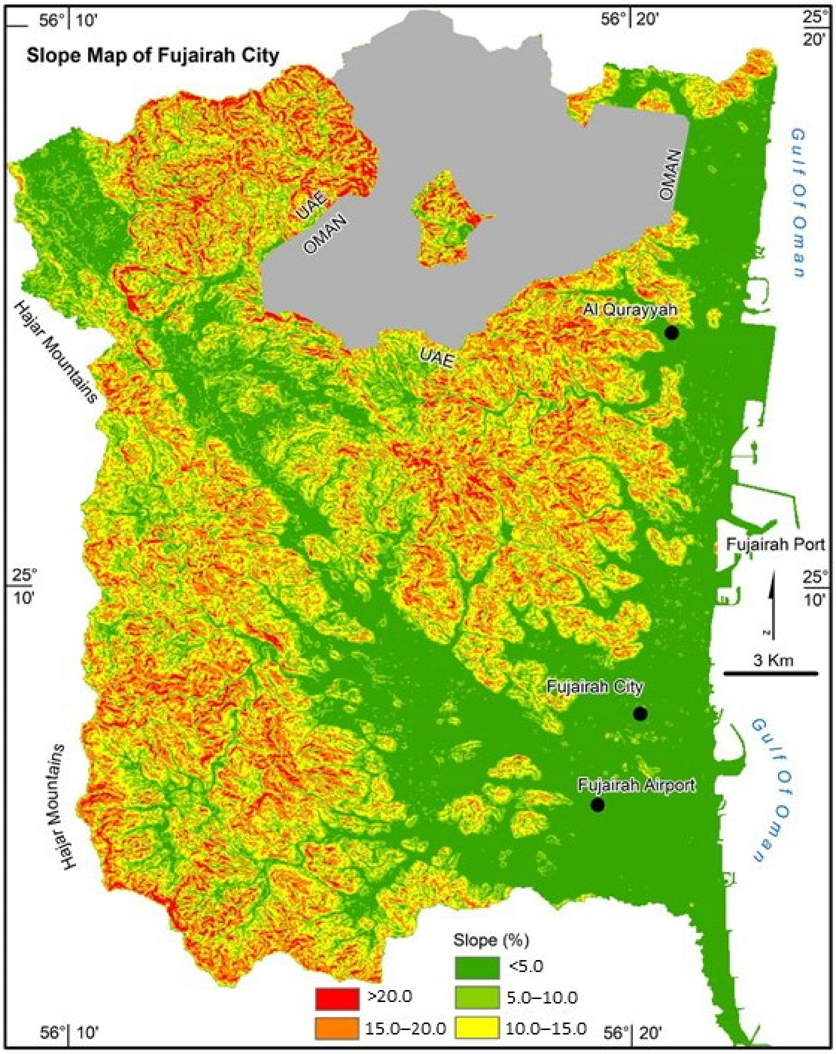

Figure 10. Slope map of Fujairah City.

4.1.4. Drainage Density

A key concept in hydrological analysis is drainage density, determined as the total drainage length to the basin area. The drainage density is influenced by the permeability, the capacity of surface materials to erode, vegetation, slope, and time. Overland flow caused by inadequate drainage might choke drainage and water channels [98]. Equation 1 is used to calculate the drainage density:

$$D = L/A \tag{1}$$

where D is the water drainage density, L is the drainage channel's overall length, and A is the water area. Higher drainage density values are significantly correlated with a lower likelihood of floods in the region since it denotes greater surface runoff, while lower drainage density values resemble higher vulnerability to flash floods. The prepared drainage density map is shown in Figure 11 using the line density command in the ArcGIS

Hydrology module. The drainage density map of the study area is generated from the drainage network layer. According to [99], regions with higher drainage densities produce more surface runoff than regions with lower drainage densities. Accordingly, the drainage density, a crucial element for creating runoff [100,101], may depend on the expansion of flood risk.

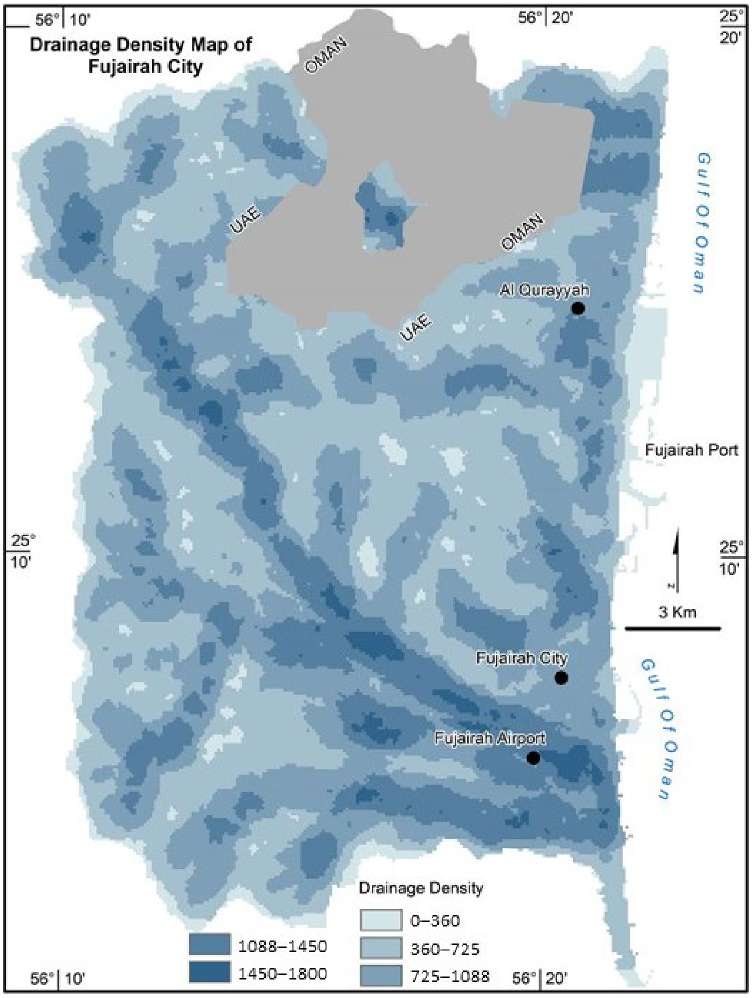

Figure 11. Drainage density map of Fujairah City.

4.1.5. Land Use/Land Cover

The structure of land use, the distribution of land cover, and its temporal evolution can all have a significant impact on an area's flood frequency [102,103]. The land use of an area has a significant impact on hydrological responses at different times, according to [103]. Therefore, ref. [104] showed that changes in land use can increase a region's likelihood of flooding. This paper creates a detailed LULC map utilizing on-screen digitization of Sentinel-2 data pertaining to 2023, as shown in Figure 12. There were mainly ten categories were identified on the LULC map, and their areas are represented in Table 2, namely Builtup-Residential, Builtup-Commercial, Builtup-Residential/Plantation, Builtup-Under development, Builtup-Mining, Barren Lands, Builtup-Oil storage areas, Airport, Fujairah Port, Beaches and Hajar Mountains. The Hajar Mountains occupy around 403 km^2, while the residential and plantation areas comprise 52 km^2, and mining areas include 14 km^2. Fujairah port has a total area of 11.7 km^2 and an oil storage area of another 5.7 km^2. In all these areas, Built-up residential and plantation areas, Fujairah Port, Commercial areas, airports, oil storage areas, and beaches are given a high-risk value of 5. In contrast, Under-development areas, plantation areas, under development areas are given a risk value of 4, mining areas into 3, barren lands 2, and mountains 1, as shown in Table 3.

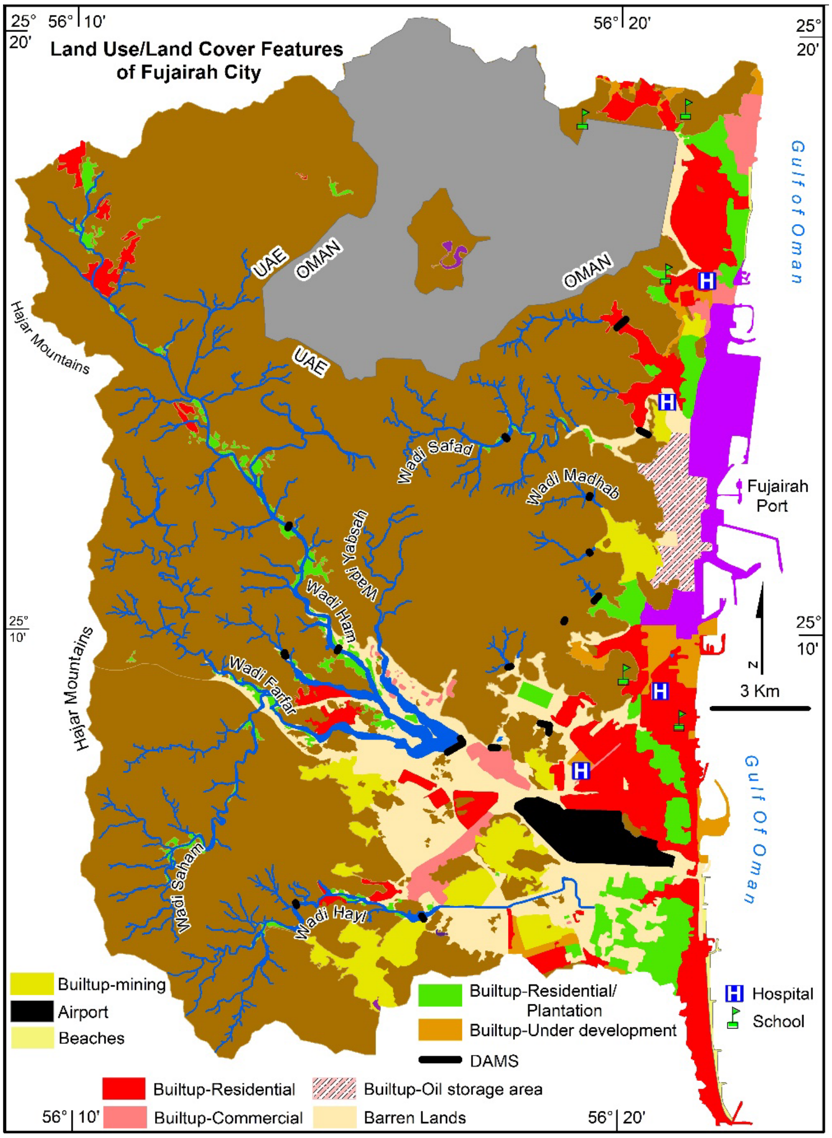

Figure 12. Land Use/Land Cover Map of Fujairah City.

Table 2. Land use land cover classification of the study area.

S. No	Land Use/Land Cover Class	Area (Km^2)
1	Builtup-Residential	31.54
2	Builtup-Commercial	6.48
3	Builtup-Residential/Plantation	20.76
4	Builtup-Under development	6.06
5	Builtup-Mining	14.26
6	Barren Lands	40.20
7	Builtup-Oil storage areas	5.79
8	Airport	5.9
9	Beaches	0.91
10	Fujairah Port	11.7
11	Hajar Mountains	403.82

Table 3. Weights, classes, and scores for map layers.

S. No	Map Layer	Classes	Rank	Weightage (%)
1	Rainfall in mm	80–140	3	18.4
		140–150	4	
		160>	5	
2	Drainage Density	0–360	5	14.3
		360–725	4	
		725–1088	3	
		1088–1450	2	
		1450–1800	1	
3	Elevation in M	0–50	5	12.2
		50–150	4	
		150–250	3	
		250–350	2	
		>350	1	
4	Slope in (%)	<5	5	13.4
		5–10	4	
		10–15	3	
		15–20	2	
		>20	1	
5	Geology	Igneous and Metamorphic	2	10.1
		Permian to Cretacious Sedimentary	2	
		Quaternary Alluvium in Wadis, Plains, Sands	4	
		Quaternary Coastal deposits	5	
6	Geomorphology	Alluvial Plains	4	9.0
		Coastal Plains	5	
		Flood Plain	4	
		Beaches	5	
		Mountains	1	
7	Land Use and Land Cover	Builtup-Residential	5	14.5
		Builtup-Commercial	5	
		Builtup-Residential/Plantation	4	
		Builtup-Under development	4	
		Builtup-Mining	3	
		Barren Lands	2	
		Builtup-Oil storage areas	5	
		Airport	5	
		Beaches	5	
		Fujairah Port	5	
		Hajar Mountains	1	
8	Soil	Aquisalids	5	8.1
		Haplocalcids	4	
		Torriorthents	3	
		Rock outcrops	2	
		Mountains	1	

4.1.6. Geology

Due to geological variance, a region's temporal flood has a high potential to change the wadi profile [105], and it can be regarded as a significant factor since it increases the severity of a flood occurrence [106,107]. Additionally, a region's geology can provide important details about the frequency of paleo-flood occurrences [108]. The infiltration rate and a rock's permeability are strongly correlated. To prevent floods, impermeable rocks encourage surface drainage. The study area's geology map was created based on past research by [109,110], and it is split into four primary geological types: Igneous and metamorphic rocks from the Jurassic to the Cretaceous Period; sedimentary rocks from the Permian to the Cretaceous Period; alluvium from the Quaternary Period in Wadis, plains, and sands; and Quaternary Coastal Deposits (Figure 13). Finally, larger infiltration rates will result from a geological formation with higher permeability, whereas higher surface runoff rates will result from an impermeable layer.

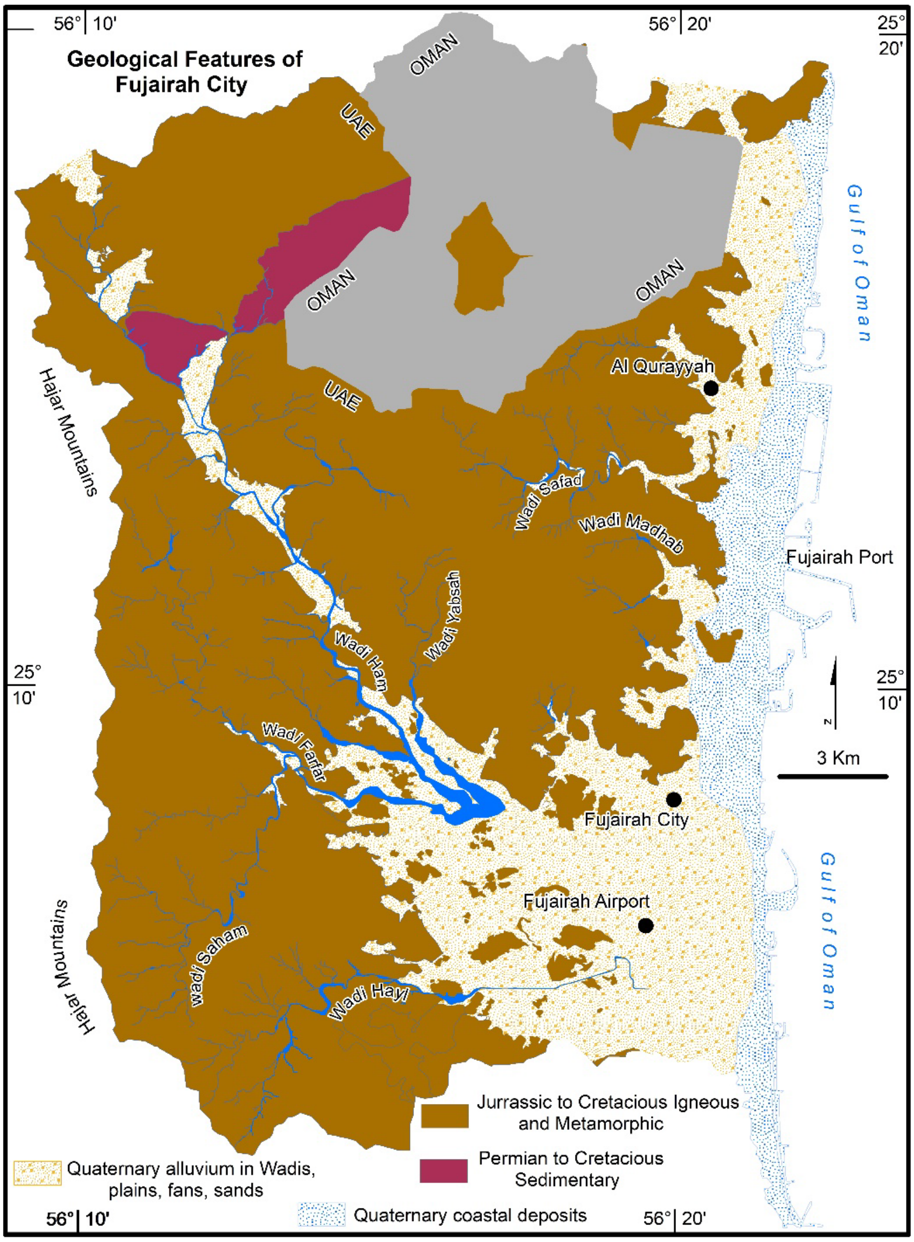

Figure 13. Geology map of Fujairah City.

4.1.7. Geomorphology

According to [109,111,112] Bullard and Livingstone (2002), Nash (2000), Colin F. Pain et al. (2014), the interplay of wind and water is a major element in the geomorphology of arid regions and has a significant impact on long-term landscape evolution in these locations. Additionally, fine silt is transported to alluvial areas by rain and floods, where it can be altered by aeolian processes [111]. Like how dust and sand are transported by wind, they can be carried by water in channels or as a surface wash in alluvial and sloped environments.

Therefore, one of the most crucial factors in assessing flash flood susceptibility is geomorphological analysis. It is essential to the management of water resources and aids in a variety of planning and development tasks, such as managing floodplains, building recharge structures, and rerouting stormwater, among others. In the research region, there are primarily five geomorphic features detailed in Figure 14 that was chosen as a reference from [109]. Wadis, Flood Plains, and Alluvial Plains are examples of fluvial landforms. Along with beaches, Coastal Plains comprise the other major landform in the study region.

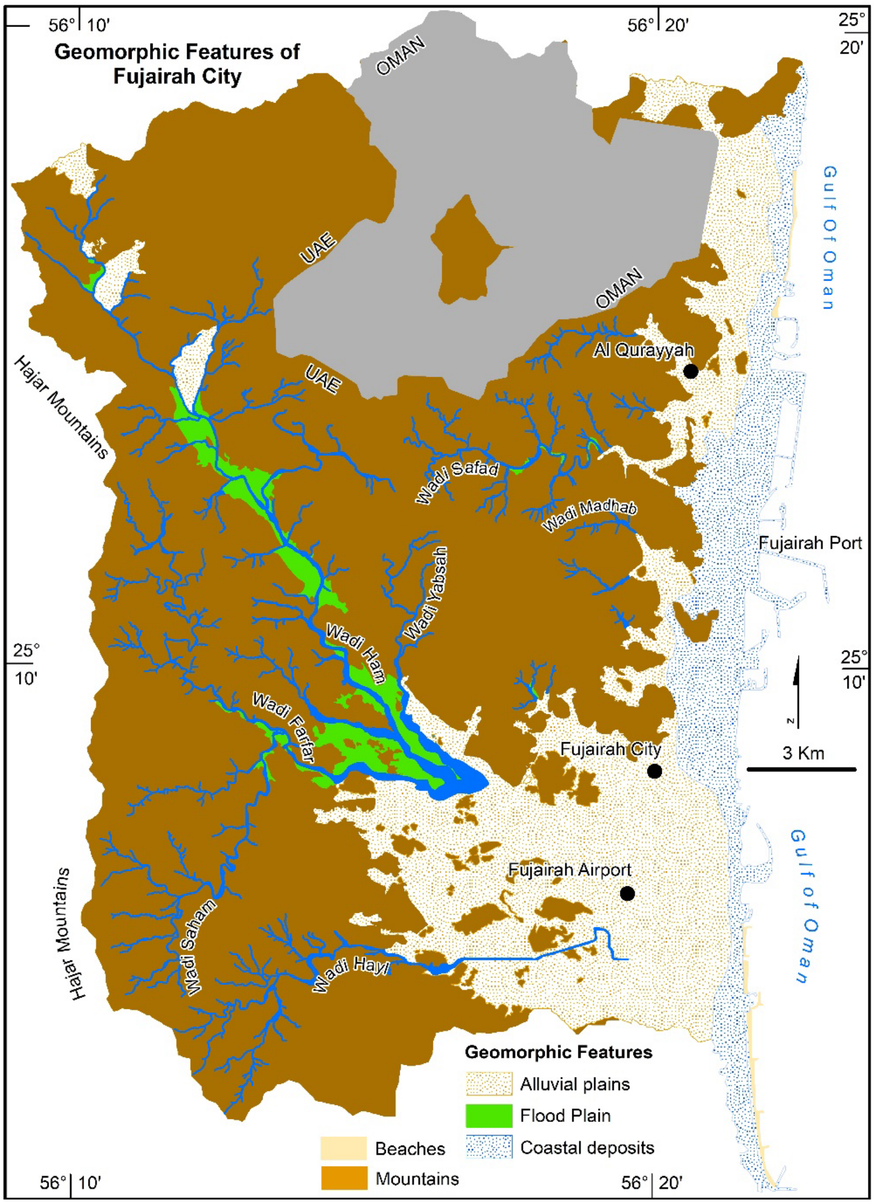

Figure 14. Geomorphology map of Fujairah City.

4.1.8. Soil

A natural resource that directly affects floods is soil because it regulates how much water can permeate the soil and is the main element of the hydrological cycle [113], as a result, how much water flows [114]. In dry locations with severe water scarcity, soil information and maps are crucial for decision-making [115]. They provide a wealth of information on its environmental applications and potential concerns. The ability of soils to infiltrate water and behave as sponges will be significantly influenced by their structure and infiltration capacity. Different types of soils hold and infiltrate water differently, impacting flood susceptibility [116]. Reduced soil infiltration capacity leads to increased surface runoff, which raises the risk of flooding. Flooding can occur when water is delivered at a pace that exceeds the soil's capacity for infiltration [117]. This is because the water rushes down the slope at a rapid rate. The created soil map from [115] is depicted in Figure 15. The study area's soil comprises five types: Aquisalids, Haplocalcids, Torriorthents, Rock outcrops, and Mountains.

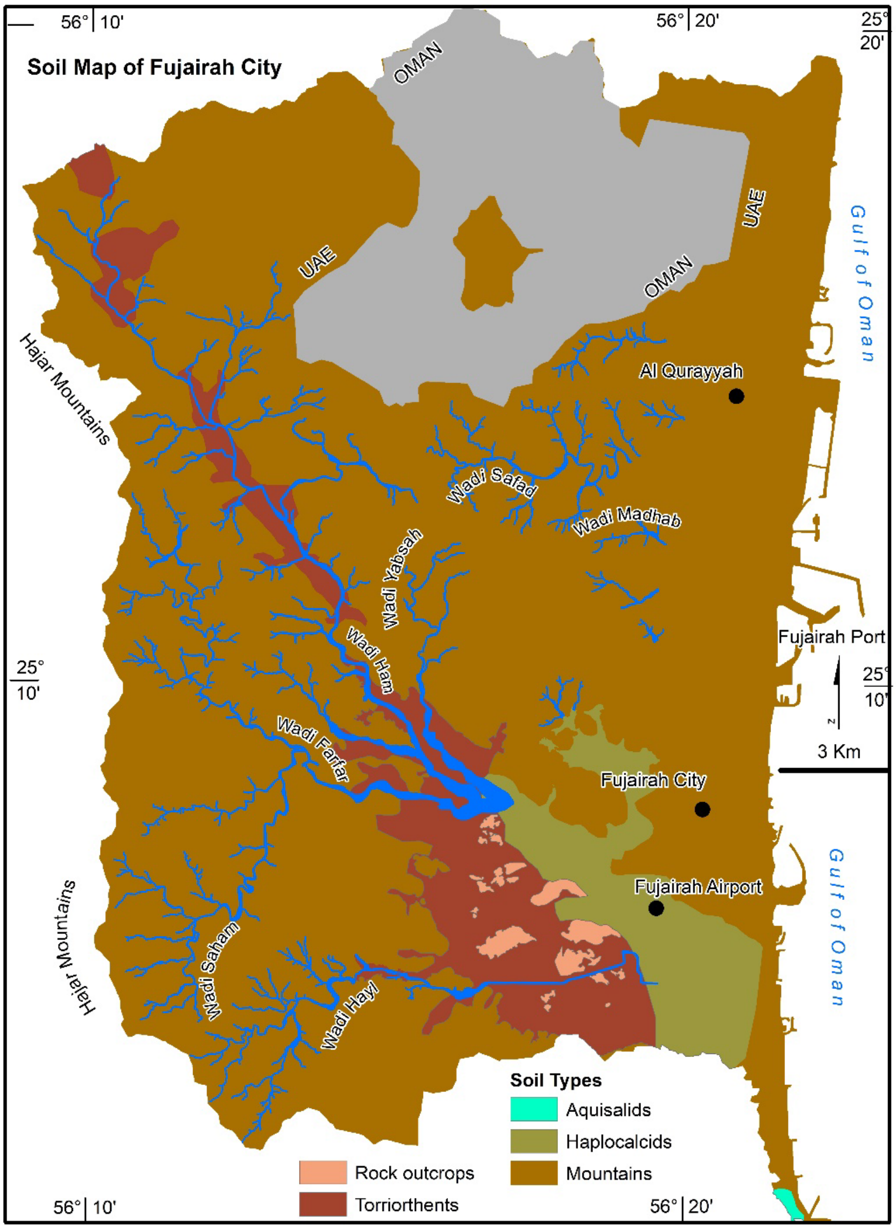

Figure 15. Soil map of Fujairah City.

In coastal regions, aquisalids are extremely salinity-rich and poorly drained soils. These soils are located toward the southwest of the research region and encompass an area of 0.362 km^2. In addition to having a high concentration of salts, some of these soils also have a high concentration of gypsum. Salt concentrations are intense towards the surface due to capillary rise and water evaporation. The extreme salinity of these soils causes them to be physiologically dry despite groundwater, which only allows salt-tolerant plant species to grow there.

Haplocalcids are a type of soil where the upper layer of the subsoil contains calcium carbonate. These soils cover 26.33 km^2 in the research area, with the majority of them situated in the center to the northwest region. These soil types can readily absorb surface water since they are typically sandy or loamy. 12% of the city of Fujairah is covered by these types of soils.

Most torriorthents contain more than 35% by volume of gravel. They are found in wadis within mountain valleys, alluvial fans, and plains next to mountains. Other Torriorthents are found on wadis or alluvial plains farther away from the mountains. They are usually sandy and have little to no gravel, but within 100 cm, there may be one or more strata with a loamy texture. The term “rock outcrops” refers to regions of rock outcrop surrounded by soils rather than the vast amounts of rock outcrop that make up the mountains. It comprises rounded hills with low relief and steep, rocky hills in some places. The 3.643 km^2 area of this map unit is covered by various outcrops made of sandstone, conglomerate, limestone, gypsum, ophiolite, and gabbro, among other rock types.

5. Results

Evaluation of Probable Flash Flood Vulnerable Zones

In assessing the risk of flash flooding, GIS is increasingly important. A spatial database is created using ArcGIS 10.4. The study of raster overlays is crucial in assembling the data needed to portray the phenomena. One of the simplest ways to join distinct layers is by using “Yes” or “No” rules from Boolean logic. Most Boolean logical-based overlay processes used in GIS do not consider the fact that variables may not be equally important and that threshold value determinations are sometimes arbitrary. The mathematical Overlay approach was therefore used to quantify the analysis’s parameters. The result is a raster layer with a value assigned to each grid cell due to the productive overlay procedure.

By combining the spatial data of rainfall, drainage density, elevation, slope, LULC, geology, geomorphology, and soil, a map of flood risk zones has been created. The parameter’s weight value is displayed as a percentage between 0% and 100%. The list of the intended parameters, their weights, and their ranks are shown in Table 3. The class values are ranked from 1 to 5 per scientific norms and presumptions after calculating the criteria value ranges [118]. Rankings were given from 1 to 5, with 5 representing the most significant element and 1 representing the least important. The proper weights were assigned based on the features and characteristics of the strata shown in Table 3. Figure 16 illustrates the creation of the flash flood vulnerable map for the study area using information from Table 3. The very high, high, moderate, low, and very low vulnerable zones, which account for 11.7%, 16.6%, 1.9%, 25.5%, and 44.3% of the research area, respectively, are shown on the flood-vulnerable map. Because mountains with heights greater than 80 m above mean sea level encompass most of the study area, 71.7% of it falls under moderate to very low vulnerable zones. The remaining 28.3% comprises high and very highly vulnerable areas. This includes the heavily inhabited, low-lying districts overlooking the Gulf of Oman in Fujairah City, which has encroached into topographically delicate territory prone to flash floods. Additionally, as seen in Figure 3, the steady increase of built-up areas in the Fujairah City region expands the area of impermeable infrastructure, which reduces infiltration and increases runoff in the event of significant rainfall over a brief period.

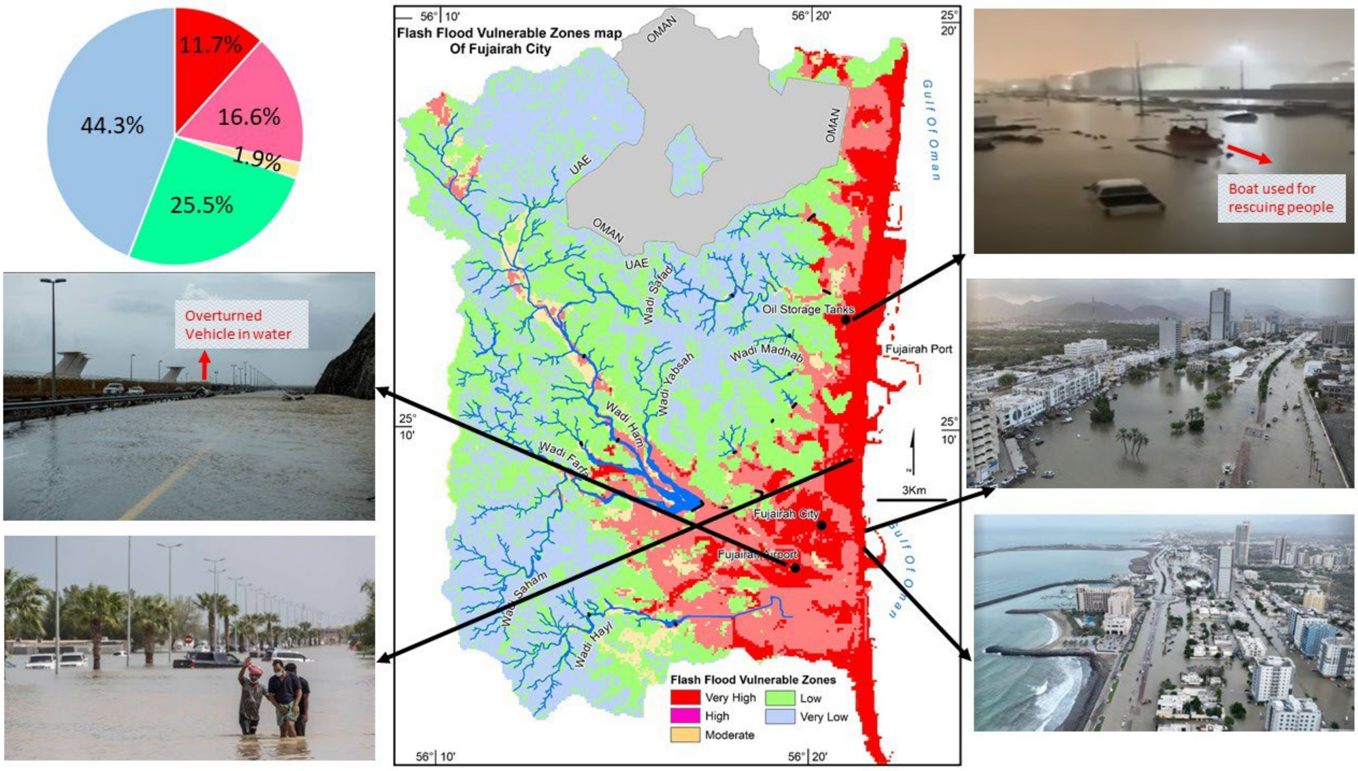

Figure 16. Flash flood vulnerable zones of Fujairah City.

Nearly 90% of the images from earlier flood events taken on the field, discovered in areas with highly vulnerable zones for flooding (Figure 16), were used to confirm the accuracy of the flash flood vulnerability map along with the reference from [4,32]. This shows that the GIS model output and the earlier flash flood occurrences had a significant degree of consistency. The map of flash flood vulnerable zones is a useful tool for planning flood defences and safeguarding the safety of persons residing in extremely high and very highly vulnerable areas. For instance, since it was discovered that more vulnerable areas are located along the low coastal plains, which regrettably are areas of high population density, preventive measures, such as the incorporation of planning regulations, the avoidance of development near highly vulnerable areas, the construction of embankments, raising public awareness, and the establishment of early warning systems by the installation of flow meters with alarms, can be taken into consideration. By adding additional storage dams, raising the heights of the current ones, and clearing the silt from them, more water can be saved, groundwater can be recharged, and people can be protected from flash floods [119,120]. To use the estimated 150 million m^3 per year from 15 major catchment areas in the UAE, the Ministry of Environment and Water built 113 recharge and storage dams [121]. To lessen the impact of flooding, an early warning system for flash floods is essential. Additionally, remote sensing data might supplement rain gauge data for real-time precipitation estimation [122–125]. This would allow researchers to determine whether a rainstorm event will suddenly cause low-lying areas to flood.

6. Discussion

The results of this study concur with those from previous studies employing machine learning [4] and weighted analytical techniques [32]. They determined that among the chosen factors, elevation and slope carried the most weight. Flash floods were mostly caused by elevation, with slope and rainfall coming in second and third. Another study from Ethiopia, by [126], determined that slope is the main reason for flash floods. Additionally, ref. [51] stated that the primary characteristics of their study include rainfall, DD, elevation, and slope. The findings of previous research [127] and ref. [98] demonstrated the critical role that elevation and slope play in influencing the movement of the overflow route. Also [32] included LULC in their analysis. The current analysis emphasizes assigning high weightage for rainfall, DD, elevation, slope, and LULC while considering all the previous studies.

To develop flash flood risk zones, weighted sum overlay analysis fusion methodologies were used. These can forecast flood risk areas thanks to the many different classification criteria. A flash flood vulnerability map was produced by incorporating eight conditional parameters through GIS-based weighted overlay analysis, normalization, and expert opinion technique, as discussed in previous research [128–130]. A larger weight indicates high flooding vulnerability. Lower weight levels, on the other hand, suggest that flooding is less likely to happen. The outcome map was separated into five zones using the natural break method: very high, high, moderate, low, and very low (Figure 16), covering areas of 55 km^2, 78 km^2, 9.3 km^2, 120 km^2, 207 km^2 (Figure 16). Fujairah City has been identified as one of the locations with the highest risk of flooding. This results from the Fujairah city's quick development, encroaching on topographically delicate regions vulnerable to flash floods. In addition, building and road construction in urban areas expands the area of impervious infrastructure, which reduces infiltration and increases runoff, leading to flash floods in the event of heavy rain that falls over a short time. The much more significant causes of flood vulnerability in these areas are human activities that result in considerable changes in the geometry of the watershed, such as elevation changes in the topography, existing drainage modifications, and a rise in the number of impervious surfaces in the City area (Figure 3). All of these factors have raised the risk of floods and flooding of essential infrastructure, which increases the chance of fatalities and financial loss [2]. Despite the high-risk area, change detection maps showed the significant changes that have occurred in urban and vegetation areas since 1990 (Figure LULC alterations). 2010 to 2023 saw a significant improvement in Fujairah City's infrastructure.

In general, flood risk maps are helpful for local citizens, decision-makers, and competent authorities. They can help select the best flood risk reduction measures for watersheds [131–133]. It is simpler to locate the danger areas with flood risk mapping. Additionally, there will be consistency in deciding how and where to reduce urban expansion in the risk zones with a methodical technique like weighted overlay analysis. The growth of urban areas near floodplain areas and the presence of many facilities may enhance the flood intensity. The findings of this study demonstrated that urbanization has an impact on hydrological processes as well, reducing groundwater infiltration and increasing runoff.

6.1. Hazard Management, Field Observations and Recommendations

We learnt that the Wadi Ham South Dam experienced water overflowing during the floods of July 2022 (Figure 5), which caused the neighboring areas to flood. We have thus examined the wadis that are to blame for this flood in this regard. Two wadis, wadi Farfar and Wadi Saham, where Wadi Saham joins with Wadi Farfar and later both the wadis empties into the Wadi Ham main dam, are to blame for the increased flood water accumulation in the Wadi Ham south dam. Wadi Saham has a width of 67 m before joining Wadi Farfar, and Wadi Farfar has 236 m width before reaching the Wadi Ham main Dam.

After thorough field visits, these two wadis have no breaker dams or artificial lakes, so they are the source of the additional flood water. Furthermore, Wadi Saham's bed slope (Figure 17c) is quite steep, causing the water to surge into Wadi Fafar before rejoining the Wadi Ham main dam. The field photos were collected during the most recent floods in July 2022 (Figure 5). The Wadi Safad and Wadi Madhab both have steep slopes (Figure 17e,f) that will cause the flow strength to grow and flood the downstream areas. Due to the abrupt power of the water from upstream that defines the steep slopes in the wadi bed, there were destroyed roads and culverts downstream of Wadi Safad (Figure 18).

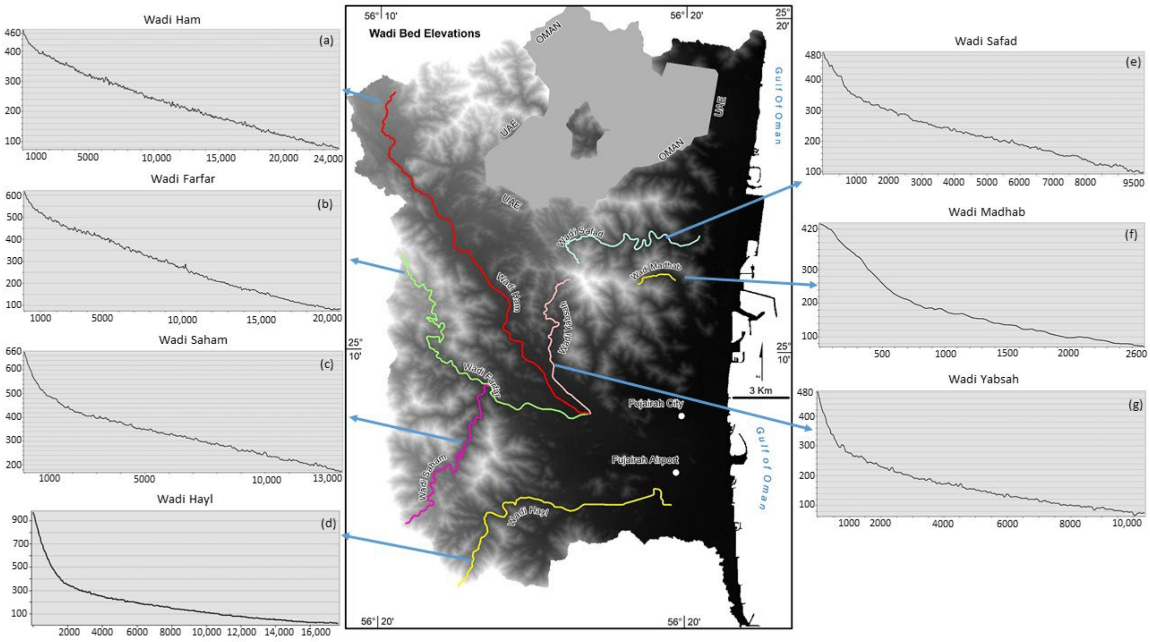

Figure 17. Wadi bed elevations for different wadis in Fujairah City (**a**)Wadi Ham (**b**) WadiFarfar (**c**)Wadi Saham (**d**)Wadi Hayl (**e**)Wadi Safad (**f**)Wadi Madhab (**g**)Wadi Yabsah.

Figure 18. Showing the eroded culverts and road downstream of Wadi Safad.

Before reaching the Wadi Ham main dam, Wadi Ham has a 330 m width, which is claimed to be the widest of all the wadis in the analysis of Wadi bed widths. Its width is roughly 45 m, close to the starting point. The Wadi Safad has a maximum width of 119 m close to the Safad Dam, and as you descend toward the downstream breaker dam near Al Qurayyah, that breadth increases to 280 m.

Monitoring flood-prone areas can reduce the likelihood of flooding [134], and flood mitigation strategies can be divided into non-structural and structural approaches [134,135]. Non-structural measures do not require engineering, such as boosting preparation through early warnings, controlling land use and development, planning and managing flood control reservoirs, and more [135,136]. In-depth ecosystem-specific methods, including restoring natural conditions or conventional measures like dams and levees can be used as structural defence tactics [135]. In addition, structural improvements may be crucial for controlling dangerous floods and managing water [137,138].

According to [134,139], successful flood mitigation techniques should consider the following factors: (1) a proper flood control implementation strategy; (2) a suitable site for facility installation; (3) a suitable facility size; and (4) efficient facility maintenance and operation. Most of the roads and other infrastructure in Fujairah City have been built across wadis that encircle the main city. Although complete flood protection is impractical, the risk of a flood disaster could be decreased by (1) reducing exposure by stopping or shifting development activities in floodplains and other high-hazard areas, (2) reducing vulnerability by establishing resilient infrastructure standards and designs, and (3) reducing the hazard itself, in some cases, by building flood mitigation measures.

6.2. Essential Physical Structural Procedures

Structured mitigation strategies can be divided into scattered and concentrated strategies according to the spatial scale. Distributed structural measures for flood mitigation have been considered in several previous research [140–145]. According to [141,145], the major objective of dispersed structures is to ease the flow peak and store extra floodwaters upstream of wadis to lessen the discharge in downstream areas. Fujairah has implemented several methods to reduce flash floods, including integrating retention and breaker dams and man-made lakes, resulting in water management and flood mitigation. Following a thorough analysis of all the wadis in Fujairah City by researchers, it was discovered that 15 breaker dams have 4 m in height built on three Wadis, in addition to 2 main dams of 12 m each built on the wadi Ham and wadi Safad (Figure 1). Also, there should be one breaker dam built each on the Wadi Saham and Wadi Farfar. Therefore, to control flash floods and water harvesting, which in turn helps to improve the groundwater aquifers of Fujairah City, some breaker dams and artificial lakes should be proposed based on the expected volume of flood water, risk and hazard degree, and their return periods.

6.3. Necessary Solutions without Any Physical Structures

By altering land use, issuing early warnings, and lowering flood susceptibility and exposure, non-structural flood control strategies have been widely used to lower the flow peak [136,146–148]. Additionally, socioeconomic developments and governmental structures impact how effective non-structural flood control techniques are [149]. On the other hand, non-structural control measures offer adaptable flood mitigation strategies for considering changes in Wadi systems, climate change, and socioeconomic effects, which might impede the establishment of a sustainable environment [150].

7. Conclusions

Numerous flash floods have affected Fujairah City and its residents, some of which have been quite catastrophic and have left lasting harm in their wake, as was shown by the most recent flooding on 28 July 2022. After carefully examining the various geomorphic features of the research region, it became apparent that seven wadis flowed into Fujairah City and that roughly 17 dams, including two significant dams and additional breaker dams, had been built to hold water. To analyze and manage flash flood hazards, it is crucial to create a flash flood hazard map. After normalization and weighting by implementing expert opinions, several parameters, mostly derived from remote sensing data, such as slope, elevation, land use, land cover, geomorphology, geology, soil, rainfall, and drainage density, were combined to map flood-vulnerable areas. The information made it possible to assess the impact of the floods on Fujairah City and identify the areas that were most at risk. The Fujairah City Flash Flood susceptible zones model identified very high susceptible areas (11.72%), highly vulnerable areas (16.63%), moderate (1.9%), low (25.58%), and very low (44.13%) vulnerability.

Because it is largely steep terrain, the western section of the study area is less susceptible to flash floods. Due to the flat coastal plain and impermeable regions, the eastern portion, where the metropolitan areas are situated, is extremely vulnerable to flooding. The model findings were verified and compared to the flood that occurred on 28 July 2022, and they nearly matched the vulnerability map's final results. As approximately 27% of the study region, which includes mining sites, underdevelopment areas, residential areas, and other built-up areas, is subject to significant hazards due to floods, the research's findings can help to lessen the risks that flood catastrophes offer to the local people. The weighted overlay method and GIS analysis used in this study to create the flood vulnerable map provide municipality officials with crucial information that they can use to explain the risks of flooding and develop emergency preparedness and mitigation strategies for various target groups, particularly for residents of high-risk neighborhoods.

Using maps and satellite images procured at distinct points in time and at different scales can lead to attribute and positional mistakes, leading to technical limits in any GIS-related procedures. As a result of generalization, there can be probable inaccuracies in the classification of land uses. For instance, even though they are categorized as built-up residential areas under the law of the majority, built-up regions also include many green spaces. The Shuttle Radar Topography Mission (SRTM) is the foundation for the elevation data. One-arc second data (30 m) is the resolution of the source data cells. Since no other topographical data were available, the SRTM data, which is typically not appropriate for flood modeling [151], was used in this work.

Furthermore, it is inaccurate to categorize elevation based just on bare ground. If an area has a good drainage system, especially in metropolitan areas, it may not be true that low ground has a high likelihood of flooding. The growth of new highways and urban areas, as well as climate change, will cause changes to the flash flood vulnerability map over time [152]. As a result, the present flood vulnerability map created here should only be used as a basic guide. It should not be utilized to make long-term decisions.

Author Contributions: Conceptualization, S.P.; methodology, S.P.; software, S.P.; validation, S.P., A.A., A.A.E. and M.S.; formal analysis, S.P., A.A.E. and M.S.; investigation, S.P., A.S., S.B.M. and F.L.R.; resources, S.P., S.B.M. and F.L.R.; data curation, S.P. and A.S.; writing—original draft preparation, S.P.; writing—review and editing, S.P. and A.A.; visualization, S.P.; supervision, S.P., M.S. and A.A.E.; project administration, S.P., A.S., S.B.M. and F.L.R. All authors have read and agreed to the published version of the manuscript.

Funding: The National Water and Energy Center of the United Arab Emirates University has supported this research. The authors thank the journal's editorial board and reviewers for their professional assistance.

Data Availability Statement: Not applicable.

Conflicts of Interest: The authors declare no conflict of interest.

References

1. Abdelkareem, M. Targeting flash flood potential areas using remotely sensed data and GIS techniques. *Nat. Hazards* **2017**, *85*, 19–37. [CrossRef]
2. Pham, T.; Avand, M.; Janizadeh, S.; Phong, T.V.; Al-Ansari, N.; Ho, L.S.; Das, S.; Le, H.V.; Amini, A.; Bozchaloei, S.K.; et al. GIS Based Hybrid Computational Approaches for Flash Flood Susceptibility Assessment Binh. *Water* **2020**, *12*, 683. [CrossRef]
3. Waqas, H.; Lu, L.; Tariq, A.; Li, Q.; Baqa, M.F.; Xing, J.; Sajjad, A. Flash flood susceptibility assessment and zonation using an integrating analytic hierarchy process and frequency ratio model for the Chitral District, Khyber Pakhtunkhwa, Pakistan. *Water* **2021**, *13*, 1650. [CrossRef]
4. Elmahdy, S.; Ali, T.; Mohamed, M. Flash flood Susceptibility Modeling and Magnitude Index using Machine Learning and Geohydrological Models: A Modified Hybrid Approach. *Remote Sens.* **2020**, *12*, 2695. [CrossRef]

5. Taylor, J.; Man, L.K.; Davies, M.; Clifton, D.; Ridley, I.; Biddulph, P. Flood management: Prediction of microbial contamination in large-scale floods in urban environments. *J. Environ. Int.* **2011**, *37*, 1019–1029. [CrossRef]
6. Oruonye, E.D. Socio-economic impact assessment of flash flood in Jalingo metropolis, Taraba State, Nigeria. *Int. J. Environ. Sci.* **2012**, *1*, 135–140.
7. Zhang, D.; Quan, J.; Zhang, H.; Wang, F.; Wang, H.; He, X. Flash flood hazard mapping: A pilot case study in Xiapu River Basin, China. *Water Sci. Eng.* **2015**, *8*, 195–204. [CrossRef]
8. Abdelkareem, M.; El-Baz, F. Analyses of optical images and radar data reveal structural features and predict groundwater accumulations in the central Eastern Desert of Egypt. *Arab. J. Geosci.* **2015**, *8*, 2653–2666. [CrossRef]
9. Abdelkareem, M.; Al-Arifi, N. The use of remotely sensed data to reveal geologic, structural, and hydrologic features and predict potential areas of water resources in arid regions. *Arab. J. Geosci.* **2021**, *14*, 704. [CrossRef]
10. Mansour, A.M.; El-Sadek, M.S. Risk Assessment of Climate Change on the Coastal area of Quseir, Red Sea, Egypt. In *Climate Change Management through Adaptation and Mitigation*; Privitera, R., La Rosa, D., Pappalardo, V., Martinico, F., Eds.; Open Access Creative Commons license CC BY-NC-ND 4.0 International Attribution; Maggioli Editore: Santarcangelo di Romagna, Italy, 2021; pp. 64–69.
11. Kron, W. Keynote lecture: Flood risk = hazard × exposure × vulnerability. In *Flood Defence 2002*; Science Press Ltd.: New York, NY, USA, 2002; pp. 82–97.
12. Yin, J.; Yu, D.; Yin, Z.; Liu, M.; He, Q. Evaluating the impact and risk of pluvial flash flood on intra-urban road network: A case study in the city center of Shanghai, China. *J. Hydrol.* **2016**, *537*, 138–145. [CrossRef]
13. Bui, D.T.; Panahi, M.; Shahabi, H.; Singh, V.P.; Shirzadi, A.; Chapi, K.; Khosravi, K.; Chen, W.; Panahi, S.; Li, S.; et al. Novel Hybrid Evolutionary Algorithms for Spatial Prediction of Floods. *Sci. Rep.* **2018**, *8*, 15364. [CrossRef]
14. Tehrany, M.S.; Pradhan, B.; Jebur, M.N. Flood susceptibility analysis and its verification using a novel ensemble support vector machine and frequency ratio method. *Stoch. Environ. Res. Risk Assess* **2015**, *29*, 1149–1165. [CrossRef]
15. Jackson, J.A.; Bates, R. *Glossary of Geology: Alexandria*; American Geological Institute: Alexandria, VA, USA, 1997; p. 769.
16. Sen, Z. *Wadi Hydrology*; CRC Press: New York, NY, USA, 2008.
17. Khan, Q.; Kalbus, E.; Zaki, N.; Mohamed, M.M. Utilization of social media in floods assessment using data mining techniques. *PLoS ONE* **2022**, *17*, e0267079. [CrossRef] [PubMed]
18. Subraelu, P.; Sefelnasr, A.; Yagoub, M.M.; Sherif, M.; Ebraheem, A.A.; Raj Sekhar, A.; Nageswara Rao, K. Global warming cli-mate change and sea level rise: Impact on land use land cover features along UAE coast through remote sensing and GIS. *J. Ecosyst. Ecography* **2022**, *12*, 329.
19. El Bastawesy, M.; White, K.; Nasr, A. Integration of remote sensing and GIS for modelling flash floods in Wadi Hudain catchment, Egypt. *Hydrol. Process.* **2009**, *23*, 1359–1368. [CrossRef]
20. UNISDR. *Terminologies on Disaster Risk Reduction—United Nations International Strategy for Disaster Reduction Geneva, Switzerland*; UNISDR: Geneva, Switzerland, 2009.
21. Guha-Sapir, D.; Below, R.; Hoyois, P. EM-DAT: The CRED/OFDA International Disaster Database. 2016. Available online: https://www.emdat.be/ (accessed on 17 April 2023).
22. De Vries, A.J.; Ouwersloot, H.G. Identification of tropical-extratropical interactions and extreme precipitation events in the Middle East based on potential vorticity and moisture transport. *J. Geophys. Res. Atmos.* **2018**, *123*, 861–881. [CrossRef]
23. Al Khatry, A.; Helmi, T. The effect of Gonu cyclone on recharging groundwater aquifers—Sultanate of Oman. In Proceedings of the 1st International Conference on Water Resources and Climate Change in the MENA Region, Muscat, The Sultanate of Oman, 2–4 November 2008; Available online: https://www.researchgate.net/publication/329034781_The_Effect_of_Gonu_Cyclone_on_Recharging_Groundwater_Aquifers_-_Sultanate_of_Oman (accessed on 21 July 2023).
24. Al Barwani, A. Flash flood mitigation and harvesting Oman case study. In Proceedings of the 1st International Symposium on Flash Floods (ISFF), Kyoto, Japan, 14–15 October 2015.
25. Abdeldayem, O.M.; Eldaghar, O.; Mostafa, M.K.; Habashy, M.M.; Hassan, A.A.; Mahmoud, H.; Morsy, K.M.; Abdelrady, A.; Peters, R.W. Mitigation Plan and Water Harvesting of Flashflood in Arid Rural Communities Using Modelling Approach: A Case Study in Afouna Village, Egypt. *Water* **2020**, *12*, 2565. [CrossRef]
26. Aly, M.M.; Refay, N.H.; Elattar, H.; Morsy, K.M.; Bandala, E.R.; Zein, S.A.; Mostafa, M.K. Ecohydrology and flood risk management under climate vulnerability in relation to the sustainable development goals (SDGs): A case study in Nagaa Mobarak Village, Egypt. *Nat. Hazards* **2022**, *112*, 1107–1135. [CrossRef]
27. Murata, M.; Ozawa, H. Post Aswan High Dam flash floods in Egypt: Causes, consequences and mitigation strategies. *Bull. Cent. Collab. Community Naruto Univ. Educ.* **2015**, *29*, 173–186.
28. Abdel-Fattah, M.; Kantoush, S.A. Rainfall-runoff modeling for extreme flash floods in Wadi Samail, Oman. *J. Jpn Soc. Civ. Eng. Ser. B1 Hydraul. Eng.* **2018**, *74*, I_691–I_696. [CrossRef]
29. Jordan: Flash Floods Kill 12 and Force Tourists to Flee. 2018. Available online: https://www.theguardian.com/world/2018/nov/10/jordan-flash-floods-kill-eleven-and-forced-tourists-to-flee (accessed on 18 May 2023).
30. Al-Qudah, K.A. Floods as water resource and as a hazard in arid regions: A case study in southern Jordan. *Jordan J. Civ. Eng.* **2011**, *5*, 148–161.
31. Youssef, A.M.; Sefry, S.A.; Pradhan, B.; Alfadail, E.A. Analysis oncauses of flash flood in Jeddah city (Kingdom of Saudi Arabia) of 2009 and 2011 using multi-sensor remote sensing data and GIS. *Geomat. Nat. Hazards Risk* **2016**, *7*, 1018–1042. [CrossRef]

32. Yagoub, M.M.; Alsereidi, A.A.; Mohamed, E.A.; Periyasamy, P.; Alameri, R.; Aldarmaki, S.; Alhashmi, Y. Newspapers as a validation proxy for GIS modeling in Fujairah, United Arab Emirates: Identifying flood prone areas. *Nat. Hazards* **2020**, *104*, 111–141. [CrossRef]
33. Flossmann, A.I.; Manton, M.; Abshaev, A.; Bruintjes, R.; Murakami, M.; Prabhakaran, T.; Yao, Z. Review of advances in precipitation enhancement research. *Bull. Am. Meteorol. Soc.* **2019**, *100*, 1465–1480. [CrossRef]
34. Malik, S.; Bano, H.; Rather, R.A.; Ahmad, S. Cloud Seeding; Its Prospects and Concerns in the ModernWorld-A Review. *Int. J. Pure App. Biosci.* **2018**, *6*, 791–796. [CrossRef]
35. Mazroui, A.A.; Farrah, S. The UAE Seeks Leading Position in Global Rain Enhancement Research. *J. Weather Modif.* **2017**, *49*, 54–55. [CrossRef]
36. Almheiri, K.B.; Rustum, R.; Wright, G.; Adeloye, A.J. Study of Impact of Cloud-Seeding on Intensity-Duration-Frequency (IDF) Curves of Sharjah City, the United Arab Emirates. *Water* **2021**, *13*, 3363. [CrossRef]
37. Jin, H.; Liang, R.; Wang, Y.; Tumula, P. Flood—Runoff in semiarid and sub-humid regions, a case study: A simulation of Jianghe Watershed in Northern China. *Water* **2015**, *7*, 5155–5172. [CrossRef]
38. Tehrany, M.S.; Kumar, L.; Jebur, M.N.; Shabani, F. Evaluating the application of the statistical index method in flood susceptibility mapping and its comparison with frequency ratio and logistic regression methods. *Geomat. Nat Hazards* **2019**, *10*, 79–101. [CrossRef]
39. Yariyan, P.; Avand, M.; Abbaspour, R.A.; Haghighi, T.A.; Costache, R.; Ghorbanzadeh, O.; Janizadeh, S.; Blaschke, T. Flood susceptibility mapping using an improved analytic network process with statistical models. *Geomat. Nat. Hazards Risk* **2020**, *11*, 2282–2314. [CrossRef]
40. Chen, N.; Zhang, Y.; Wu, J.; Dong, W.; Zou, Y.; Xu, X. The trend in the risk of flash flood hazards with regional development in the Guanshan River Basin China. *Water* **2020**, *12*, 1815. [CrossRef]
41. Vivekanandan, N. Comparison of probability distributions in extreme value analysis of rainfall and temperature data. *Environ. Earth Sci.* **2018**, *77*, 201. [CrossRef]
42. Monsef, H.A.E. A mitigation strategy for reducing flood risk to highways in arid regions: A case study of the El-Quseir–Qena highway in Egypt. *J. Flood Risk Manag.* **2018**, *11*, S158–S172. [CrossRef]
43. Sujatha, E.R.; Selvakumar, R.; Rajasimman, U.A.B.; Victor, R.G. Morphometric analysis of subwatershed in parts of Western Ghats, South India using ASTER DEM. *Geomat. Nat. Hazard Risk* **2013**, *6*, 326–341. [CrossRef]
44. Bhatt, S.; Ahmed, S.A. Morphometric analysis to determine floods in the Upper Krishna Basin using Cartosat DEM. *J. Geocarto Int.* **2014**, *29*, 878–894. [CrossRef]
45. Abdel-Fattah, M.; Kantoush, S.; Sumi, T. Integrated management of flash flood in wadi system of Egypt: Disaster prevention and water harvesting. In Proceedings of the 1st International Symposium on Flash Floods in Wadi System—Disaster Risk Reduction and Water Harvesting of Flash Floods in the Arab Regions, Kyoto, Japan, 14–15 October 2015; Available online: https://repository.kulib.kyoto-u.ac.jp/dspace/bitstream/2433/210044/1/a58b0p54.pdf (accessed on 22 July 2023).
46. Farhan, Y.; Anaba, O.; Salim, A. Morphometric Analysis and flashfloods assessment for drainage basins of the RasEnNaqb Area South Jordan Using GIS. *J. Geosci. Environ. Protect.* **2016**, *4*. [CrossRef]
47. Szewrański, S.; Kazak, J.; Szkaradkiewicz, M.; Sasik, J. Flood Risk Factors in Suburban Area in the Context of Climate Change Adaptation Policies—Case Study of Wroclaw, Poland. *J. Ecol. Eng.* **2015**, *16*, 13–18. [CrossRef]
48. Recanatesi, F.; Petroselli, A.; Ripa, M.N.; Leone, A. Assessment of storm water runoff management practices and BMPs under soil sealing: A study case in a peri-urban watershed of the metropolitan area of Rome (Italy). *J. Environ. Manag.* **2017**, *201*, 6–18. [CrossRef]
49. El-Rawy, M.; Elsadek, W.M.; De Smedt, F. Flash flood susceptibility mapping in Sinai, Egypt using hydromorphic data, principal component analysis and logistic regression. *Water* **2022**, *14*, 2434. [CrossRef]
50. Zhao, G.; Pang, B.; Xu, Z.; Peng, D.; Xu, L. Assessment of urban flood susceptibility using semi-supervised machine learning model. *Sci. Total Environ.* **2019**, *659*, 940–949. [CrossRef]
51. Periyasamy, P.; Yagoub, M.M.; Sudalaimuthu, M. Flood vulnerable zones in the rural blocks of Thiruvallur districts, South India. *Geoenviron. Disasters* **2018**, *5*, 21.
52. Vojtek, M.; Vojtekov, J. Flood hazard and flood risk assessment at the local spatial scale: A case study. *Geomat. Nat Hazards Risk* **2016**, *7*, 19731992. [CrossRef]
53. Arabameri, A.; Saha, S.; Mukherjee, K.; Blaschke, T.; Chen, W.; Ngo, P.T.T.; Band, S.S. Modeling Spatial Flood using Novel Ensemble Artificial Intelligence Approaches in Northern Iran. *Remote. Sens.* **2020**, *12*, 3423. [CrossRef]
54. Forkuo, E.K. Flood hazard mapping using Aster image data with GIS. *Int. J. Geomat. Geosci.* **2011**, *1*, 932–950. Available online: https://www.ipublishing.co.in/jggsvol1no12010/EIJGGS2051.pdf (accessed on 20 June 2023).
55. Quirós, E.; Gagnon, A.S. Validation of flood risk maps using open source optical and radar satellite imagery. *Trans. GIS* **2020**, *24*, 1208–1226. [CrossRef]
56. Getahun, Y.S.; Gebre, S.L. Flood hazard assessment and mapping of flood inundation area of the Awash River Basin in Ethiopia using GIS and HEC-GeoRAS/HEC-RAS Model. *J. Civil. Environ. Eng.* **2015**, *5*, 179. Available online: https://www.omicsonline.org/open-access/flood-hazard-assessment-and-mapping-offloodinundation-area-of-the-awash-river-basin-in-ethiopia-using-gis-and-hecgeorashecras--model-2165-784X-1000179.php?aid=57721 (accessed on 19 May 2023).

57. Samanta, S.; Koloa, C.; Pal, D.K.; Palsamanta, B. Flood risk analysis in lower part of Markham River based on multi-criteria decision approach (MCDA). *Hydrology* **2016**, *3*, 29. [CrossRef]
58. Kelly, M.; Schwarz, I.; Ziegelaar, M.; Watkins, A.B.; Kuleshov, Y. Flood Risk Assessment and Mapping: A Case Study from Australia's Hawkesbury-Nepean Catchment. *Hydrology* **2023**, *10*, 26. [CrossRef]
59. Sefelnasr, A.; Ebraheem, A.A.; Faiz, M.A.; Shi, X.; Alghafli, K.; Baig, F.; Al-Rashed, M.; Alshamsi, D.; Ahamed, M.B.; Sherif, M. Enhancement of Groundwater Recharge from Wadi Al Bih Dam, UAE. *Water* **2022**, *14*, 3448. [CrossRef]
60. Sherif, M.; Sefelnasr, A.; Al Rashed, M.; Alshamsi, D.; Zaidi, F.K.; Alghafli, K.; Baig, F.; Al-Turbak, A.; Alfaifi, H.; Loni, O.A.; et al. A Review of Managed Aquifer Recharge Potential in the Middle East and North Africa Region with Examples from the Kingdom of Saudi Arabia and the United Arab Emirates. *Water* **2023**, *15*, 742. [CrossRef]
61. Al-Dogom, D.; Al-Ruzouq, R.; Kalantar, B.; Schuckman, K.; Al-Mansoori, S.; Mukherjee, S.; Al-Ahmad, H.; Ueda, N. Geospatial Multicriteria Analysis for Earthquake Risk Assessment: Case Study of Fujairah City in the UAE. *J. Sensors* **2021**, *2021*, 6638316. [CrossRef]
62. Subraelu, P.; Yagoub, M.M.; Sefelnasr, A.; Nageswara, K.; Allamsatti, R.S.; Ebraheem, A.A.; Sherif, M. Sea-level Rise and Coastal Vulnerability: A preliminary Assessment of UAE Coast through Remote Sensing and GIS. *J. Coast. Zone Mang.* **2021**, *24*, 477–480.
63. Elmahdy, S.I.; Mohamed, M.M.; Ali, T. Land Use/Land Cover Changes Impact on Groundwater Level and Quality in the Northern Part of the United Arab Emirates. *Remote Sens.* **2020**, *12*, 1715. [CrossRef]
64. Al-Rashed, M.F.; Sherif, M.M. Water Resources in the GCC Countries: An Overview. *Water Resour. Manag.* **2000**, *14*, 59–75. [CrossRef]
65. Sherif, M.; Almulla, M.; Shetty, A.; Chowdhury, R. Analysis of rainfall, PMP and drought in the United Arab Emirates. *Int. J. Clim.* **2014**, *34*, 1318–1328. [CrossRef]
66. Ghazanfar, S.A.; Fisher, M. (Eds.) *Vegetation of the Arabian Peninsula*; Springer: Berlin/Heidelberg, Germany, 1998. [CrossRef]
67. Sherif, M.; Mohamed, M.; Kacimov, A.; Shetty, A. Assessment of groundwater quality in the northeastern coastal area of UAE as precursor for desalination. *Desalination* **2011**, *273*, 436–446. [CrossRef]
68. Subraelu, P.; Ebraheem, A.A.; Sherif, M.; Sefelnasr, A.; Yagoub, M.M.; Rao, K.N. Land in Water: The Study of Land Reclamation and Artificial Islands Formation in the UAE Coastal Zone: A Remote Sensing and GIS Perspective. *Land* **2022**, *11*, 2024. [CrossRef]
69. Sengupta, D.; Chen, R.; Meadows, M.E. Building beyond land:An overview of coastal land reclamation in16 global megacities. *Appl. Geogr.* **2018**, *90*, 229–238. [CrossRef]
70. Shah, S.M.H.; Mustaffa, Z.; Teo, F.Y.; Imam, M.A.H.; Yusof, K.W.; Al-Qadami, E.H.H. A review of the flood hazard and risk management in the South Asian Region, particularly Pakistan. *Sci. Afr.* **2020**, *10*, e00651. [CrossRef]
71. Gan, B.R.; Liu, X.N.; Yang, X.G.; Wang, X.K.; Zhoua, J.W. The impact of human activities on the occurrence of mountain flood hazards: Lessons from the 17 August 2015 flash flood/debris flow event in Xuyong County, South-Western China. *Geomat. Nat. Hazards Risk* **2018**, *9*, 816–840. [CrossRef]
72. Gulf Today. Fujairah's Flood. 2022. Available online: https://www.gulftoday.ae/news/2022/07/29/at-least-six-dead-due-to-uae-floods (accessed on 22 July 2023).
73. The National News. 2022. Available online: https://www.thenationalnews.com/uae/2022/07/29/water-was-up-to-my-shoulders-fujairah-residents-recall-aftermath-of-major-floods (accessed on 22 July 2023).
74. Aliyev, E. Fujairah Bunker Ops Remain Disrupted after Flood. 2022. Available online: https://www.argusmedia.com/en/news/2355927-fujairahbunker-ops-remain-disrupted-after-flood (accessed on 22 July 2023).
75. Alhefeiti FR, M.O.; Alblooshi MA, M.; Abdalla RY YY, A.; Kalathingal MS, H.; Mirza, S.B.; Ridouane, F.L. Investigation of the effects of heavy rain and flood in Emirates of Fujairah–UAE and Construction and Compilation of Flood Map and Elevation Chart Using State of the Art GIS Technologies. *Int. J. Dev. Res.* **2022**, *12*, 58827–58831.
76. Kursah, M.B. Application of GIS in flood detection for road infrastructure planning in north-eastern corridor of northern Ghana. *Int. J. Appl. Sci. Technol.* **2013**, *3*, 94–106.
77. Goel, N.K.; Kurothe, R.S.; Mathur, B.S.; Vogel, R.M. A derived flood frequency distribution for correlated rainfall intensity and duration. *J. Hydrol.* **2000**, *228*, 56–67. [CrossRef]
78. Zhang, Y.; Smith, J.A. Space–time variability of rainfall and extreme flood response in the Menomonee River Basin, Wisconsin. *J. Hydrometeorol.* **2003**, *4*, 506–517. [CrossRef]
79. Rozalis, S.; Morin, E.; Yair, Y.; Price, C. Flash flood prediction using an uncalibrated hydrological model and radar rainfall data in a Mediterranean watershed under changing hydrological conditions. *J. Hydrol.* **2010**, *394*, 245–255. [CrossRef]
80. Hong, H.; Panahi, M.; Shirzadi, A.; Ma, T.; Liu, J.; Zhu, A.; Chen, W.; Kougias, I.; Kazakis, N. Flood susceptibility assessment in Hengfeng area coupling adaptive neuro-fuzzy inference system with genetic algorithm and differential evolution. *Sci. Total. Environ.* **2018**, *621*, 1124–1141. [CrossRef]
81. Zhao, G.; Pang, B.; Xu, Z.; Yue, J.; Tu, T. Mapping flood susceptibility in mountainous areas on a national scale in China. *Sci. Total Environ.* **2018**, *615*, 1133–1142. [CrossRef]
82. Kay, A.L.; Jones, R.G.; Reynard, N.S. RCM rainfall for UK flood frequency estimation. II. Climate change results. *J. Hydrol.* **2006**, *318*, 163–172.
83. Segond, M.L.; Wheater, H.S.; Onof, C. The significance of spatial rainfall representation for flood runoff estimation: A numerical evaluation based on the Lee catchment, UK. *J. Hydrol.* **2007**, *347*, 116–131. [CrossRef]

84. Tehrany, M.S.; Pradhan, B.; Jebur, M.N. Spatial prediction of flood susceptible areas using rule based decision tree (DT) and a novel ensemble bivariate and multivariate statistical models in GIS. *J. Hydrol.* **2013**, *504*, 69–79. [CrossRef]
85. Tehrany, M.S.; Pradhan, B.; Mansor, S.; Ahmad, N. Flood susceptibility assessment using GIS-based support vector machine model with different kernel types. *Catena* **2015**, *125*, 91–101. [CrossRef]
86. Bui, D.T.; Pradhan, B.; Nampak, H.; Bui, Q.T.; Tran, Q.A.; Nguyen, Q.P. Hybrid artificial intelligence approach based on neural fuzzy inference model and metaheuristic optimization for flood susceptibility modeling in a high-frequency tropical cyclone area using GIS. *J. Hydrol.* **2016**, *540*, 317–330.
87. Sherif, M.M.; Mohamed, M.M.; Shetty, A.; Almulla, M. Rainfall-Runoff Modeling of Three Wadis in the Northern Area of UAE. *J. Hydrol. Eng.* **2011**, *16*, 10–20. [CrossRef]
88. Pradhan, B. Flood Susceptible mapping and risk area delineation using logistic regression, GIS and remote sensing. *J. Spat. Hydrol.* **2009**, *9*, 1–18.
89. Botzen, W.J.W.; Aerts, J.C.J.H.; Bergh, J.C.J.M.v.D. Individual preferences for reducing flood risk to near zero through elevation. *Mitig. Adapt. Strat. Glob. Chang.* **2012**, *18*, 229–244. [CrossRef]
90. Mojaddadi, H.; Pradhan, B.; Nampak, H.; Ahmad, N.; Ghazali, A.H.B. Ensemble machine learning-based geospatial approach for flood risk assessment using multi-sensor remote sensing data and GIS. *Geomat. Nat. Hazard Risk* **2017**, *8*, 1080–1102. [CrossRef]
91. Fernandez, D.S.; Lutz, M.A. Urban flood hazard zoning in Tucuman Province, Argentina, using GIS and multicriteria decision analysis. *Eng. Geol.* **2010**, *111*, 90–98. [CrossRef]
92. Dahri, N.; Habib, A. Monte Carlo simulation-aided analytical hierarchy process (AHP) for flood susceptibility mapping in Gabes Basin (southeastern Tunisia). *Environ. Earth Sci.* **2017**, *76*, 302. [CrossRef]
93. Das, S.; Pardeshi, S.D.; Kulkarni, P.P.; Doke, A. Extraction of lineaments from different azimuth angles using geospatial techniques: A case study of Pravara basin, Maharashtra, India. *Arab. J. Geosci.* **2018**, *11*, 160. [CrossRef]
94. Das, S.; Pardeshi, S.D. Integration of different influencing factors in GIS to delineate groundwater potential areas using IF and FR techniques: A study of Pravara basin, Maharashtra, India. *Appl. Water Sci.* **2018**, *8*, 197. [CrossRef]
95. Li, K.; Wu, S.; Dai, E.; Xu, Z. Flood loss analysis and quantitative risk assessment in China. *Nat. Hazards* **2012**, *63*, 737–760. [CrossRef]
96. Zhu, Q.; Abdelkareem, M. Mapping groundwater potential zones using a knowledge-driven approach and GIS analysis. *Water* **2021**, *13*, 579. [CrossRef]
97. Çelik, H.E.; Coskun, G.; Cigizoglu, H.K.; Ağıralioğlu, N.; Aydın, A.; Esin, A.İ. The analysis of 2004 flood on Kozdere Stream in Istanbul. *Nat. Hazards* **2012**, *63*, 461–477. [CrossRef]
98. Rimba, A.B.; Setiawati, M.D.; Sambah, A.B.; Miura, F. Physical Flood Vulnerability Mapping Applying Geospatial Techniques in Okazaki City, Aichi Prefecture, Japan. *Urban Sci.* **2017**, *1*, 7. [CrossRef]
99. Kumar, P.K.; Gopinath, G.; Seralathan, P. Application of remote sensing and GIS for the demarcation of groundwater potential zones of a river basin in Kerala, southwest coast of India. *Int. J. Remote. Sens.* **2007**, *28*, 5583–5601. [CrossRef]
100. Ogden, F.L.; Raj Pradhan, N.; Downer, C.W.; Zahner, J.A. Relative importance of impervious area, drainage density, width function, and subsurface storm drainage on flood runoff from an urbanized catchment. *Water Resour. Res.* **2011**, *47*. [CrossRef]
101. Mahmoud, S.H.; Gan, T.Y. Multi-criteria approach to develop flood susceptibility maps in arid regions of Middle East. *J. Clean. Prod.* **2018**, *196*, 216–229. [CrossRef]
102. Benito, G.; Rico, M.; Sánchez-Moya, Y.; Sopeña, A.; Thorndycraft, V.R.; Barriendos, M. The impact of late Holocene climatic variability and land use change on the flood hydrology of the Guadalentín River, southeast Spain. *Glob. Planet. Chang.* **2010**, *70*, 53–63. [CrossRef]
103. García-Ruiz, J.M.; Regüés, D.; Alvera, B.; Lana-Renault, N.; Serrano-Muela, P.; Nadal-Romero, E. Flood generation and sediment transport in experimental catchments affected by land use changes in the central Pyrenees. *J. Hydrol.* **2008**, *356*, 245–260. [CrossRef]
104. Beckers, A.; Dewals, B.; Erpicum, S.; Dujardin, S.; Detrembleur, S.; Teller, J. Contribution of land use changes to future flood damage along the river Meuse in the Walloon region. *Nat. Hazards Earth Syst. Sci.* **2013**, *13*, 2301–2318. [CrossRef]
105. Reneau, S.L. Stream incision and terrace development in Frijoles Canyon, Bandelier National Monument, New Mexico, and the influence of lithology and climate. *Geomorphology* **2000**, *32*, 171–193. [CrossRef]
106. Xu, Y.; Chung, S.L.; Jahn, B.M.; Wu, G. Petrologic and geochemical constraints on the petrogenesis of Permian–Triassic Emeishan flood basalts in southwestern China. *Lithos* **2001**, *58*, 145–168. [CrossRef]
107. Kazakis, N.; Kougias, I.; Patsialis, T. Assessment of flood hazard areas at a regional scale using an index-based approach and Analytical Hierarchy Process: Application in Rhodope-Evros region, Greece. *Sci. Tot. Environ.* **2015**, *538*, 555–563. [CrossRef] [PubMed]
108. He, B.; Xu, Y.G.; Huang, X.L.; Luo, Z.Y.; Shi, Y.R.; Yang, Q.J.; Yu, S.Y. Age and duration of the Emeishan flood volcanism, SW China: Geochemistry and SHRIMP zircon U–Pb dating of silicic ignimbrites, post-volcanic Xuanwei Formation and clay tuff at the Chaotian section. *Earth Planet. Sci. Lett.* **2007**, *255*, 306–323. [CrossRef]
109. Pain, C.F.; Abdelfattah, M.A. Landform evolution in the arid northern United Arab Emirates: Impacts of tectonics, sea level changes and climate. *Catena* **2015**, *134*, 14–29. [CrossRef]
110. Sherif, M.; Sefelnasr, A.; Ebraheem, A.A.; Mulla, M.A.; Alzaabi, M.; Alghafli, K. Spatial and Temporal Changes of Groundwater Storage in the Quaternary Aquifer, UAE. *Water* **2021**, *13*, 864. [CrossRef]

111. Bullard, J.E.; Livingstone, I. Interactions between aeolian and fluvial systems in dryland environments. *Area* **2002**, *34*, 8–16. [CrossRef]
112. Nash, D.J. Arid geomorphology. *Prog. Phys. Geogr. Earth Environ.* **2000**, *24*, 425–443. [CrossRef]
113. Murad, A.; Hussein, S.; Arman, H.; Gabr, A.; Al Dhuhoori, A. The Aquifer Recharge Potential by Infiltration Tests in Arid Region, Ras Al Khaimah, United Arab Emirates. *IOP Conf. Series Earth Environ. Sci.* **2019**, *362*, 012017. [CrossRef]
114. Nicholls, N.; Wong, K.K. Dependence of rainfall variability on mean rainfall, latitude, and the Southern Oscillation. *J. Climate.* **1990**, *3*, 163–170. [CrossRef]
115. Abdelfattah, M.A.; Pain, C. Unifying regional soil maps at different scales to generate a national soil map for the United Arab Emirates applying digital soil mapping techniques. *J. Maps* **2012**, *8*, 392–405. [CrossRef]
116. Nyarko, B.K. Application of a rational model in GIS for flood risk assessment in Accra. *J. Spat. Hydrology.* **2002**, *2*, 1–14.
117. Lowery, B.; Hickey, W.J.; Arshad, M.A.; Lal, R. Soil water parameters and soil quality. In *Methods for Assessing Soil Quality*; Doran, J.W., Jones, A.J., Eds.; Reprint Soil Science Society of America: Madison, WI, USA, 1996.
118. Yagoub, M.M. Spatio—Temporal and hazard mapping of earthquake in UAE (1984–2012): Remote sensing and GIS application. *Geoenviron. Disasters* **2015**, *2*, 1–14. [CrossRef]
119. Al Abdouli, K.; Hussein, K.; Ghebreyesus, D.; Sharif, H.O. Coastal Runoff in the United Arab Emirates—The Hazard and Opportunity. *Sustainability* **2019**, *11*, 5406. [CrossRef]
120. Rizk, Z.S.; Al Sharhan, A.S. *Water Resources Perspectives: Evaluation, Management and Policy*; Alsharhan, A.S., Wood, W.W., Eds.; Elsevier Science: Amsterdam, The Netherlands, 2003; pp. 245–264.
121. Ministry of Energy, United Arab Emirates. *The United Arab Emirates: Initial National Communication to the United Nations Framework Convention on Climate Change*; Ministry of Energy, United Arab Emirates, 2006. Available online: https://unfccc.int/resource/docs/natc/arenc1.pdf (accessed on 5 April 2023).
122. Isma'il, M.; Saanyol, I.O. Application of Remote Sensing (RS) and Geographic Information Systems (GIS) in flood vulnerability mapping: Case study of River Kaduna. *Int. J. Geomat. Geosci.* **2013**, *3*, 618–627. Available online: https://citeseerx.ist.psu.edu/viewdoc/download?doi=10.1.1.421.8578&rep=rep1&type=pdf (accessed on 19 April 2023).
123. Legates, D.R. Real-time calibration of radar precipitation estimates. *Prof. Geogr.* **2000**, *52*, 235–246. [CrossRef]
124. Schumann, G.J.-P.; Bates, P.D.; Apel, H.; Aronica, G.T. (Eds.) *Global Flood Hazard: Applications in Modeling, Mapping, and Forecasting*; American Geophysical Union-Standards Information Network: Washington, DC, USA, 2018.
125. Wehbe, Y.; Ghebreyesusa, D.; Temimia, M.; Milewskib, A.; Al Mandousc, A. Assessment of the consistency among global precipitation products over the United Arab Emirates. *J. Hydrol. Reg. Stud.* **2017**, *12*, 122–135. [CrossRef]
126. Ogato, G.S.; Bantider, A.; Abebe, K.; Geneletti, D. Geographic Information System (GIS)-Based Multicriteria Analysis of Flooding Hazard and Risk in Ambo Town and Its Watershed, West Shoa Zone, Oromia Regional State, Ethiopia. *J. Hydrol. Reg. Stud.* **2020**, *27*, 100659. [CrossRef]
127. Danumah, J.H.; Odai, S.N.; Saley, B.M.; Szarzynski, J.; Thiel, M.; Kwaku, A.; Kouame, F.K.; Akpa, L.Y. Flood risk assessment and mapping in Abidjan district using multi-criteria analysis (AHP) model and geoinformation techniques, (Cote d'Ivoire). *Geoenviron. Disasters* **2016**, *3*, 1. [CrossRef]
128. Kocsis, I.; Bilașco, Ș.; Irimuș, I.A.; Dohotar, V.; Rusu, R.; Roșca, S. Flash Flood Vulnerability Mapping Based on FFPI Using GIS Spatial Analysis Case Study: Valea Rea Catchment Area, Romania. *Sensors* **2022**, *22*, 3573. [CrossRef]
129. Adlyansah, A.L. Analysis Of Flood Hazard Zones Using Overlay Method With Figused-Based Scoring Based On Geographic Information Systems: Case Study In Parepare City South Sulawesi Province. *IOP Conf. Ser. Earth Environ. Sci.* **2019**, *280*, 012003.
130. Hagos, Y.G.; Andualem, T.G.; Yibeltal, M.; Mengie, M.A. Flood hazard assessment and mapping using GIS integrated with multi-criteria decision analysis in upper Awash River basin, Ethiopia. *Appl. Water Sci.* **2022**, *12*, 148. [CrossRef]
131. Dano, U.L. An AHP-Based Assessment of Flood Triggering Factors to Enhance Resiliency in Dammam, Saudi Arabia. *GeoJournal* **2022**, *87*, 1945–1960. [CrossRef]
132. Dano, U.L. Flash Flood Impact Assessment in Jeddah City: An Analytic Hierarchy Process Approach. *Hydrology* **2020**, *7*, 10. [CrossRef]
133. Souissi, D.; Zouhri, L.; Hammami, S.; Msaddek, M.H.; Zghibi, A.; Dlala, M. GIS-Based MCDM—AHP Modeling for Flood Susceptibility Mapping of Arid Areas, Southeastern Tunisia. *Geocarto Int.* **2020**, *35*, 991–1017. [CrossRef]
134. Heidari, A. Structural master plan of flood mitigation measures. *Nat. Hazards Earth Syst. Sci.* **2009**, *9*, 61–75. [CrossRef]
135. Hansson, K.; Danielson, M. A framework for evaluation of flood management strategies. *J. Environ. Manag.* **2008**, *86*, 465–480. [CrossRef] [PubMed]
136. Shah, M.A.R.; Rahman, A.; Chowdhury, S.H. Challenges for achieving sustainable flood risk management. *J. Flood Risk Manag.* **2015**, *11*, S352–S358. [CrossRef]
137. Ho, M.; Lall, U.; Allaire, M.; Devineni, N.; Kwon, H.H.; Pal, I.; Raff, D.; Wegner, D. The future role of dams in the United States of America. *Water Resour. Res.* **2017**, *53*, 982–998. [CrossRef]
138. Al Rashed, M.; Sefelnasr, A.; Sherif, M.; Murad, A.; Alshamsi, D.; Aliewi, A.; Ebraheem, A.A. Novel concept for water scarcity quantification considering nonconventional and virtual water resources in arid countries: Application in Gulf Cooperation Council countries. *Sci. Total Environ.* **2023**, *882*, 163473. [CrossRef]
139. HEC-FDA. *Flood Damage Reduction Analysis: HEC-FDA User's Manual*; HEC: Davis, CA, USA, 1998; Volume 72.

140. Andoh, R.Y.G.; Declerck, C. A cost effective approach to stormwater management? Source control and distributed storage. *Water Sci. Technol.* **1997**, *36*, 307–311. [CrossRef]
141. Montaldo, N.; Mancini, M.; Rosso, R. Flood hydrograph attenuation induced by a reservoir system: Analysis with a distributed rainfall-runoff model. *Hydrol. Process.* **2004**, *18*, 545–563. [CrossRef]
142. Emerson, C.H.; Welty, C.; Traver, R.G. Watershed-Scale Evaluation of a System of Storm Water Detention Basins. *J. Hydrol. Eng.* **2005**, *10*, 237–242. [CrossRef]
143. Kurz, B.; Wang, X.; Silva, L.D.; Hanson, S.K.; Kurz, M.D.; Peck, W.D.; Simonsen, T.K.; Steadman, E.N. *An Evaluation of Basinwide, Distributed Storage in the Red River Basin: The Waffle®Concept*; Energy & Environmental Research Center, University of North Dakota: Grand Forks, ND, USA, 20 June 2007; Volume 23.
144. Ravazzani, G.; Gianoli, P.; Meucci, S.; Mancini, M. Assessing downstream impacts of detention basins in urbanized river basins using a distributed hydrological model. *Water Resour. Manag.* **2014**, *28*, 1033–1044. [CrossRef]
145. Thomas, N.W. Simulating the Hydrologic Impact of Distributed Flood Mitigation Practices, Tile Drainage, and Terraces in an Agricultural Catchment. Ph.D. Thesis, The Graduate College, Iowa, The University of Iowa, Iowa City, IA, USA, 2015.
146. Tapsell, S.M.; Penning-Rowsell, E.C.; Tunstall, S.M.; Wilson, T.L. Vulnerability to flooding: Health and social dimensions. *Philos. Trans. R. Soc. A Math. Phys. Eng. Sci.* **2002**, *360*, 1511–1525. [CrossRef] [PubMed]
147. White, I.; Richards, J. Planning policy and flood risk: The translation of national guidance into local policy. *Plan. Pr. Res.* **2007**, *22*, 513–534. [CrossRef]
148. Richards, J.; White, I.; Carter, J. Local planning practice and flood risk management in England: Is there a collective implementation deficit? *Environ. Urbain* **2008**, *2*, 11–20. [CrossRef]
149. Dawson, R.J.; Ball, T.; Werritty, J.; Werritty, A.; Hall, J.W.; Roche, N. Assessing the effectiveness of non-structural flood management measures in the Thames Estuary under conditions of socio-economic and environmental change. *Glob. Environ. Change* **2011**, *21*, 628–646. [CrossRef]
150. Kundzewicz, Z.W. Non-structural flood protection and sustainability. *Water Int.* **2002**, *27*, 3–13. [CrossRef]
151. Finn, H. Dam failure and inundation modeling: Test case for Ham Dam. In *Summary Report, Project Conducted by "DHI Gulf" for UAE Ministry of Environment & Water*; UAE Ministry of Environment & Water: Dubai, United Arab Emirates, 2008.
152. FEMA. Risk Mapping, Assessment and Planning (Risk MAP). 2019. Available online: https://www.fema.gov/risk-mappingassessment-and-planning-risk-map (accessed on 20 July 2023).